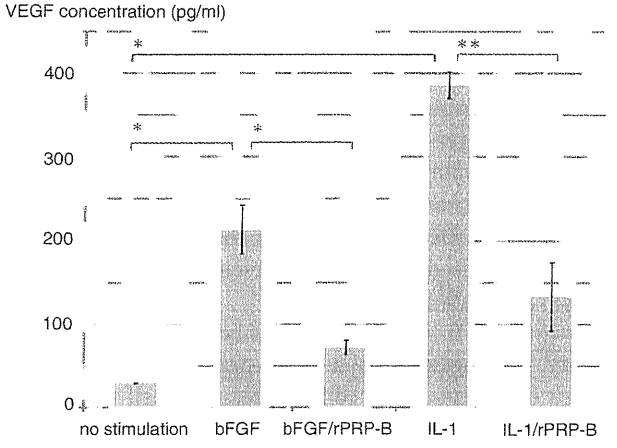

Fig. 2 Levels of VEGF in cell culture supernatants evaluated by ELISA (*$P < 0.01$; **$P < 0.005$)

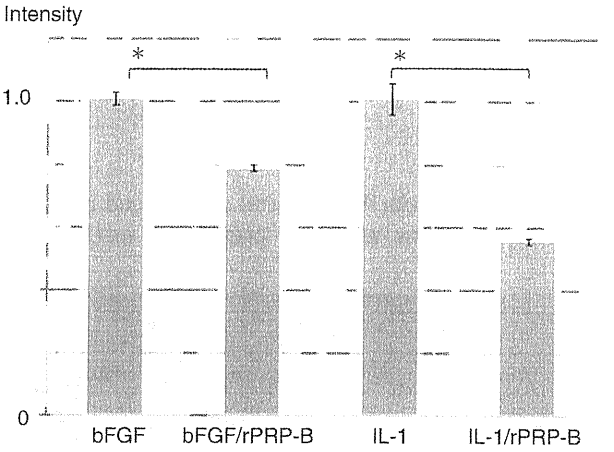

Fig. 3 Expression levels of VEGF mRNA confirmed by real-time RT-PCR (*$P < 0.05$)

Significant reductions in the expression of VEGF mRNA were also detected with rPRP-B (Fig. 3).

rPRP-B regulated collagen-induced arthritis in mice

Macroscopic evaluation of the hind paws of the rPRP-B treatment group and control mice shortly after secondary CIA immunization revealed obvious distinctions in the development of arthritis (Fig. 4). Mice treated with rPRP-B developed markedly less joint disease, as shown by a significant diminution in hind paw thickness at each time point beginning from day 27 to day 36 after injection compared with the PBS treatment group.

Histological evaluation of the CIA mouse

At 43 days after immunization, rPRP-B-injected mice displayed strikingly reduced histopathological activity of arthritis as compared with control mice (Fig. 5a–c). Inflammatory cells had infiltrated synovial tissue in untreated control mice (b), but infiltration was less severe in rPRP-B-treated mice (c). In addition, we performed detailed semi-quantitative analyses of several histopathological features. Similar to the clinical pattern, morphological signs of arthritis in drug-treated mice were dramatically reduced in comparison to control mice (Table 1).

Immunohistochemistry

Numbers of CD31-positive cells in synovia from CIA mice were significantly higher in the control group than in rPRP-B-injected mice (Fig. 6a–c). This revealed that proliferation of endothelial cells by CIA was significantly suppressed in rPRP-B mice compared to control mice. VEGF

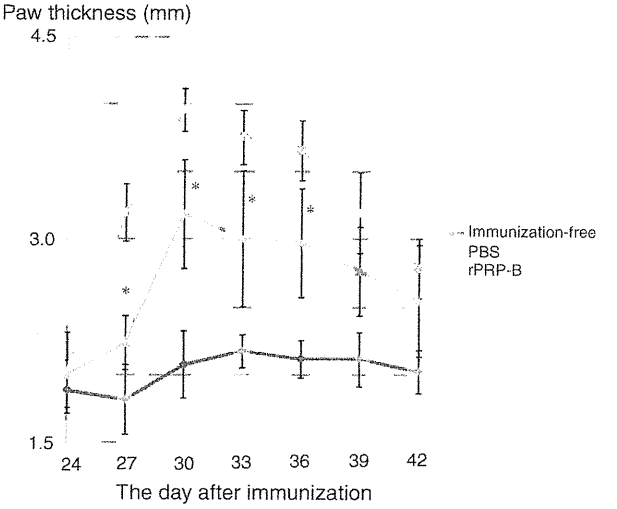

Fig. 4 Quantitative data for thickness of the swollen paw (*$P < 0.005$). Paw thickness of the site with rPRP-B injection (*filled triangles*) is significantly decreased compared to that in untreated mice (*filled quadrangles*)

expression detected by immunohistochemistry using anti-VEGF antibody was significantly reduced in a rPRP-B treated mouse compared to a control mouse (Fig. 7), suggesting that inhibition of angiogenesis by rPRP-B in the CIA mouse was at least partly attributable to VEGF suppression.

Bone destruction level was suppressed by rPRP-B treatment

Reductions in bone destruction near the metacarpal and metatarsophalangeal joints were noted on CT scans of the rPRP-B-treated group compared to controls (Fig. 8),

suggesting that rPRP-B suppresses bone destruction induced by arthritis.

Discussion

CIA mouse is reproducible and well defined, and has been extensively used to elucidate pathogenic mechanisms relevant to human RA [11]. Elevated angiogenesis in this model was also confirmed [14, 15]. The present study has shown the anti-inflammatory effects of rPRP-B as one of the candidate intrinsic anti-angiogenic factors on progression of collagen-induced arthritis. Clinical symptom, pathological findings, and radiological evaluations revealed significant suppression of collagen-induced arthritis by rPRP-B. The underlying molecular mechanisms are speculated about based on both the present in vitro study and our previous data as follows.

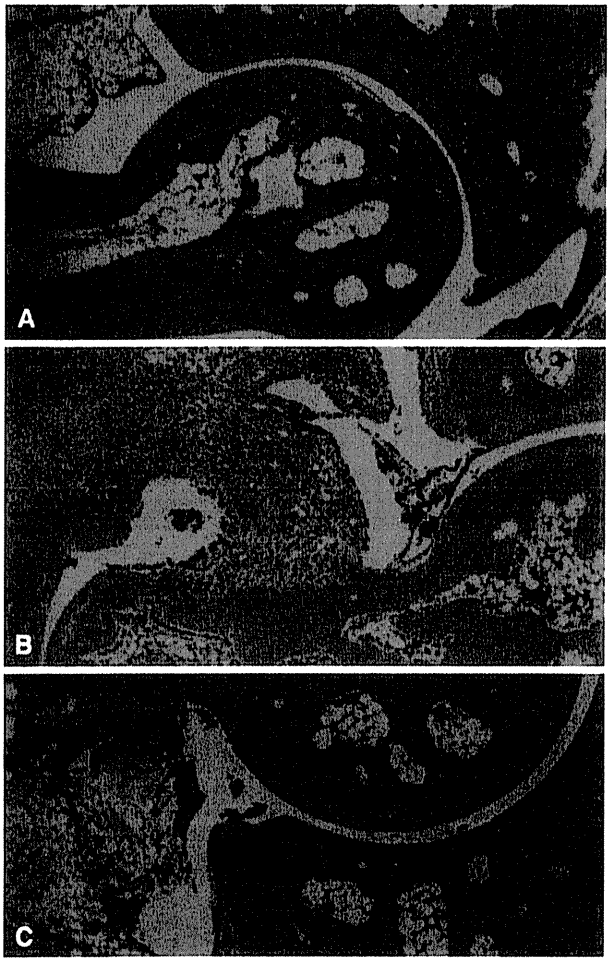

Fig. 5 Histopathological findings in mice without immunization (**a**) and in CIA mice (**b**, **c**). Histopathological evaluation revealed severe inflammation in the joint sections of untreated CIA mice (**b**). In contrast, the extent of arthritis was significantly reduced in the joints of mice with rPRP-B treatment (**c**)

First, rPRP-B could directly inhibit endothelial cell activity. Angiogenesis is a multi-step process involving various cell functions of cell proliferation, cell migration, and tube formation. We have previously shown that rPRP-B could inhibit each step of these endothelial or mural cell actions through interactions with cell surface integrin $\alpha_V\beta_3$ [3, 4, 16], suggesting that rPRP-B could have acted directly on endothelial or mural cells of CIA mice in the present study. Previous reports regarding interactions between angiogenesis in arthritis and the function of endothelial cell surface integrin support this hypothesis [17, 18]. In addition, cells that express the highest levels of integrin $\alpha_V\beta_3$ include activated macrophages, which are involved in producing proinflammatory cytokines, and osteoclasts, which mediate inflammatory osteolysis [18]. Although the initial concept of our study was control of arthritis by regulating angiogenesis through endothelial cell function, inhibition of bone destruction in rPRP-B-treated mouse and the enhanced expression of this integrin in osteoclasts led to speculation that rPRP-B could act directly on osteoclast regulation in inflammatory osteolysis. Radiological and histological analysis in the present study showed the decrease in bone destruction in the rPRP-B treatment group, supporting this speculation. For a better understanding of the mechanisms underlying the effects of rPRP-B on cells other than endothelium, further studies should be undertaken in the future.

The second key player was VEGF. VEGF is the predominant stimulator of angiogenesis [19, 20], and mediation of VEGF expression is one of the main mechanisms by which tissue vasculature is controlled under normal physiological conditions [21]. Increasing evidence of the significant role of this cytokine in the pathogenesis of RA has been emerging in recent reports [6, 22]. Consistent with these previous reports, upregulated expression of VEGF in the CIA mouse was

Table 1 Histological assessment of arthritis

	Inflammatory infiltrate*	Synovial lesions*	Cartilage destruction	Bone destruction*	Total*
PBS	2.37 ± 0.74	2.5 ± 0.53	1.63 ± 0.74	2.0 ± 0.76	8.5 ± 2.0
rPRP	1.5 ± 0.76	1.37 ± 0.92	0.88 ± 0.84	1.0 ± 0.93	4.75 ± 2.87

Data represent mean values ± SD

* $P < 0.05$

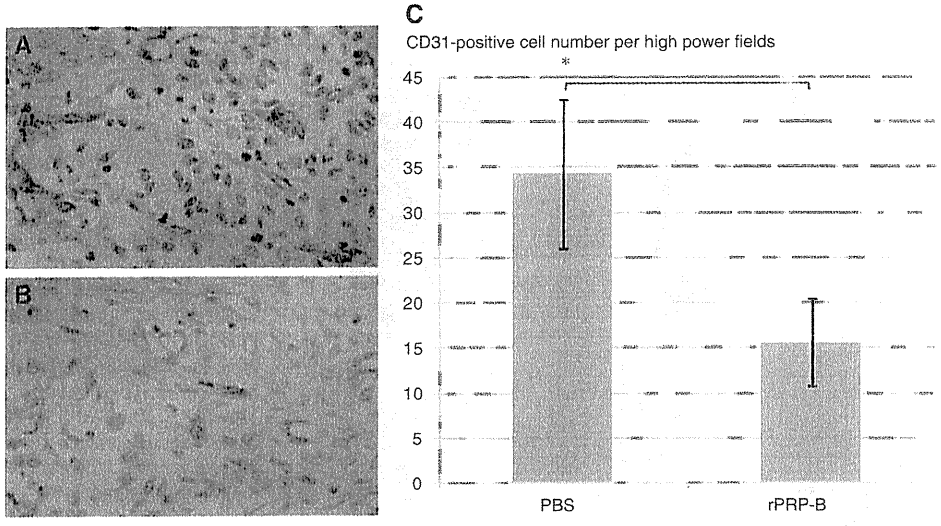

Fig. 6 Effects of rPRP-B therapy on arthritis-associated angiogenesis. Immunohistochemical staining with anti-CD31 mouse monoclonal antibody, revealing decreased vascularity in joint synovial tissue of a mouse treated with rPRP-B (**b**) compared with a control mouse (**a**). The CD31-positive cell number per high-power field in the representative specimen was significantly decreased with rPRP-B treatment mice compared with controls ($*P < 0.005$) (**c**)

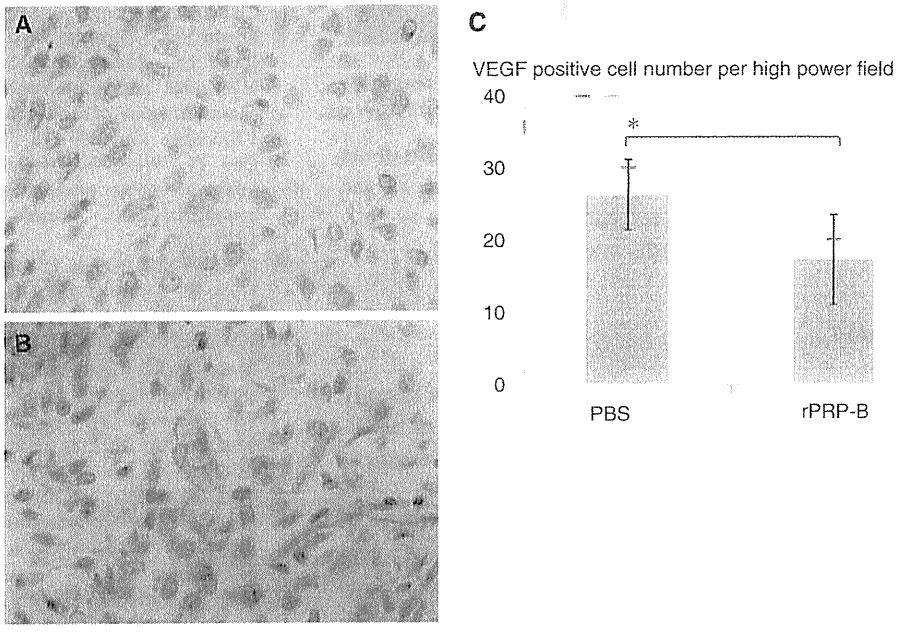

Fig. 7 Effects of rPRP-B therapy on VEGF expression in synoviocytes. Immunohistochemical staining with anti-VEGF mouse monoclonal antibody, revealing decreased VEGF expression in synovial tissue of a mouse treated with rPRP-B (**b**) compared with synovial tissue in a control mouse (**a**). The number of VEGF-positive cells per high power field in the representative specimen was significantly decreased in rPRP-B-treated mice compared to control mice ($*P < 0.005$) (**c**)

confirmed in our study. We have speculated that rPRP-B plays a regulatory role in the secretion of VEGF based on the findings from our in vivo model. As expected, downregulation of VEGF expression in rPRP-B-treated mice was confirmed. To confirm the molecular mechanisms, we confirmed the role of rPRP-B in VEGF expression by cytokine-stimulated synoviocytes. As expected, downregulation of VEGF expression by rPRP-B was confirmed in terms of both mRNA and protein levels, suggesting the molecular mechanism of downregulation in an in vivo model.

The third probable mechanism was the inhibition of direct proliferation by cytokine-stimulated synoviocytes. We have previously shown that rPRP-B exerts inhibitory effects on endothelial cell proliferation stimulated by bFGF [4]. Histological examination in the present study suggested a decrease in synoviocyte proliferation. This raises the question of whether rPRP-B has direct inhibitory effects on synoviocyte proliferation stimulated by cytokines. As expected, rPRP-B significantly inhibited cell proliferation stimulated by IL-1 or bFGF.

Thus, we could provide direct or collateral evidences supporting our hypothesis on the pathophysiological significance of rPRP-B in arthritis. However, it should be noted that some of the above-mentioned mechanisms were not directly validated in the present study. These mechanisms need to be studied in the future. In addition, recent reports suggested the probability of multiple mechanisms of resistance to anti-angiogenic therapy for cancer [23],

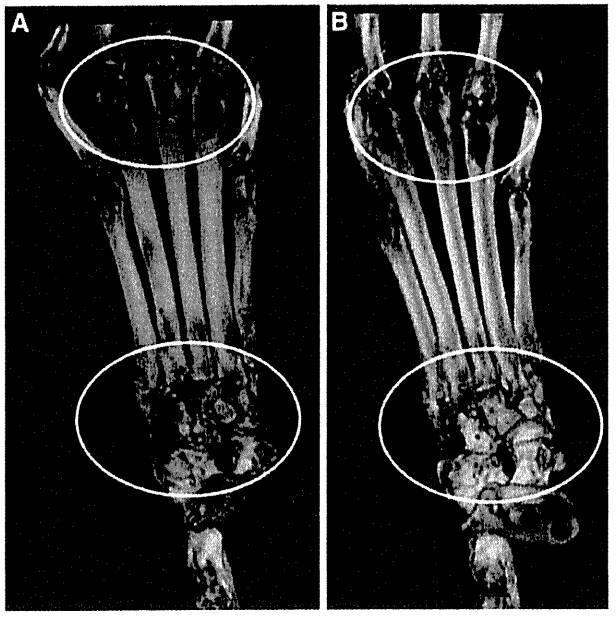

Fig. 8 Micro-CT revealing reductions in bone destruction near joints in rPRP-B-treated mice (**b**) compared with control mice (**a**) (*circle*)

suggesting the need to consider the same mechanism in the therapy for arthritis. Thus, the second limitation of the present study was that the resistance mechanism to anti-angiogenic therapy for arthritis was not validated.

Conclusion

Treatment with rPRP-B significantly decreased the severity of arthritis and improved histological findings in established CIA mice. In addition, rPRP-B reduced neovascularization and VEGF production in inflamed joints. An in vitro study revealed multi-factorial roles of rPRP-B on endothelial cell administration, VEGF secretion, and synoviocyte proliferation. These findings show that in vivo administration of rPRP-B suppresses arthritis in established CIA mice, suggesting that anti-angiogenic treatment may offer a new and additional therapeutic modality for RA.

Acknowledgments We gratefully acknowledge the technical assistance of Miyuki Murayama and Mizuho Kosuge. Financial support for this study was provided by a Grant-in-Aid for Scientific Research (C).

Conflict of interest The authors declare that they have no competing interests.

References

1. Weissbach L, Treadwell BV. A plasminogen-related gene is expressed in cancer cells. Biochem Biophys Res Commun. 1992;186:1108–14.
2. Morioka H, Weissbach L, Vogel T, Nielsen GP, Faircloth GT, Shao L, Hornicek FJ. Antiangiogenesis treatment combined with chemotherapy produces chondrosarcoma necrosis. Clin Cancer Res. 2003;9:1211–7.
3. Lewis VO, O'Reilly MS, Gehrmann M, Llinas M, Schaller J, Weissbach L. Inhibition of tumor growth by plasminogen-related protein-B. Anticancer Res. 2001;21:2287–91.
4. Morioka H, Morii T, Vogel T, Hornicek FJ, Weissbach L. Interaction of plasminogen-related protein B with endothelial and smooth muscle cells in vitro. Exp Cell Res. 2003;287: 166–77.
5. Tateno T, Ichinose A. Expression of plasminogen-related gene B varies among normal tissues and increases in cancer tissues. FEBS Lett. 1999;445:31–5.
6. Sone H, Sakauchi M, Takahashi A, Suzuki H, Inoue N, Iida K, Shimano H, Toyoshima H, Kawakami Y, Okuda Y, Matsuo K, Yamada N. Elevated levels of vascular endothelial growth factor in the sera of patients with rheumatoid arthritis correlation with disease activity. Life Sci. 2001;69:1861–9.
7. Salliot C, Dougados M, Gossec L. Risk of serious infections during rituximab, abatacept and anakinra treatments for rheumatoid arthritis: meta-analyses of randomised placebo-controlled trials. Ann Rheum Dis. 2009;68:25–32.
8. Lewis VO, Gehrmann M, Weissbach L, Hyman JE, Rielly A, Jones DG, Llinas M, Schaller J. Homologous plasminogen N-terminal and plasminogen-related gene A and B peptides: characterization of cDNAs and recombinant fusion proteins. Eur J Biochem. 1999;259:618–25.
9. Guo YL, Wang S, Colman RW. Kininostatin, an angiogenic inhibitor, inhibits proliferation and induces apoptosis of human endothelial cells. Arterioscler Thromb Vasc Biol. 2001;21: 1427–33.
10. O'Reilly MS, Boehm T, Shing Y, Fukai N, Vasios G, Lane WS, Flynn E, Birkhead JR, Olsen BR, Folkman J. Endostatin: an endogenous inhibitor of angiogenesis and tumor growth. Cell. 1997;88:277–85.
11. Rosloniec EF, Cremer M, Kang A, Myers LK. Collagen-induced arthlitis. In: Coligan JE, Kruisbeek AM, Argulies DH, Shevach EM, Strober W, editors. Current protocols in immunology. New York: Wiley; 2001. p. 15.5.1.
12. Hildner KM, Schirmacher P, Atreya I, Dittmayer M, Bartsch B, Galle PR, Wirtz S, Neurath MF. Targeting of the transcription factor STAT4 by antisense phosphorothioate oligonucleotides suppresses collagen-induced arthritis. J Immunol. 2007;178: 3427–36.
13. Chu CQ, Field M, Allard S, Abney E, Feldmann M, Maini RN. Detection of cytokines at the cartilage/pannus junction in patients with rheumatoid arthritis: implications for the role of cytokines in cartilage destruction and repair. Br J Rheumatol. 1992;31: 653–61.
14. Kurosaka D, Yoshida K, Yasuda J, Yokoyama T, Kingetsu I, Yamaguchi N, Joh K, Matsushima M, Saito S, Yamada A. Inhibition of arthritis by systemic administration of endostatin in passive murine collagen induced arthritis. Ann Rheum Dis. 2003;62:677–9.
15. Choi ST, Kim JH, Seok JY, Park YB, Lee SK. Therapeutic effect of anti-vascular endothelial growth factor receptor I antibody in the established collagen-induced arthritis mouse model. Clin Rheumatol. 2009;28:333–7.
16. Morii T, Weissbach L. Sphingosine 1-phosphate and cell migration: resistance to angiogenesis inhibitors. Biochem Biophys Res Commun. 2003;310:884–8.
17. Storgard CM, Stupack DG, Jonczyk A, Goodman SL, Fox RI, Cheresh DA. Decreased angiogenesis and arthritic disease in rabbits treated with an alphavbeta3 antagonist. J Clin Invest. 1999;103:47–54.

18. Wilder RL. Integrin alpha V beta 3 as a target for treatment of rheumatoid arthritis and related rheumatic diseases. Ann Rheum Dis 2002;61(Suppl2):96–9.
19. Jain RK. Tumor angiogenesis and accessibility: role of vascular endothelial growth factor. Semin Oncol. 2002;29:3–9.
20. Ferrara N. Role of vascular endothelial growth factor in physiologic and pathologic angiogenesis: therapeutic implications. Semin Oncol. 2002;29:10–4.
21. Ferrara N, Gerber HP, LeCouter J. The biology of VEGF and its receptors. Nat Med. 2003;9:669–76.
22. Nagashima M, Asano G, Yoshino S. Imbalance in production between vascular endothelial growth factor and endostatin in patients with rheumatoid arthritis. J Rheumatol. 2000;27: 2339–42.
23. Bergers G, Hanahan D. Modes of resistance to anti-angiogenic therapy. Nat Rev Cancer. 2008;8:592–603.

International Immunology, Vol. 23, No. 11, pp. 701–712
doi:10.1093/intimm/dxr077
Advance Access publication 21 September 2011

IL-1β and TNFα-initiated IL-6–STAT3 pathway is critical in mediating inflammatory cytokines and RANKL expression in inflammatory arthritis

Tomoaki Mori[1,2,3], Takeshi Miyamoto[1,3–6], Hideyuki Yoshida[2], Mayoko Asakawa[2], Miyuri Kawasumi[4], Takashi Kobayashi[4], Hideo Morioka[1], Kazuhiro Chiba[1], Yoshiaki Toyama[1] and Akihiko Yoshimura[2]

[1]Department of Orthopedic Surgery, [2]Department of Immunology, [3]Center for Human Metabolomic Systems Biology, [4]Keio Kanrinmaru Project and [5]Department of Integrated Bone Metabolism and Immunology, Keio University School of Medicine, 35 Shinano-machi, Shinjuku-ku, Tokyo 160-8582, Japan, [6]Precursory Research for Embryonic Science and Technology, Japan Science and Technology Agency, Kawaguchi, Saitama 332-0012, Japan

Correspondence to: T. Miyamoto; E-mail: miyamoto@z5.keio.jp

Received 19 May 2011, *accepted* 25 August 2011

Abstract

Rheumatoid arthritis (RA) is a chronic inflammatory disease that causes irreversible joint damage and significant disability. However, the fundamental mechanisms underlying how inflammation and joint destruction in RA develop and are sustained chronically remain largely unknown. Here, we show that signal transducer and activator of transcription 3 (STAT3) is the key mediator of both chronic inflammation and joint destruction in RA. We found that inflammatory cytokines highly expressed in RA patients, such as IL-1β, tumor necrosis factor alpha and IL-6, activated STAT3 either directly or indirectly and in turn induced expression of IL-6 family cytokines, further activating STAT3 in murine osteoblastic and fibroblastic cells. STAT3 activation also induced expression of receptor activator of nuclear factor kappa B ligand (RANKL), a cytokine essential for osteoclastogenesis, and STAT3 deficiency or pharmacological inhibition promoted significant reduction in expression of both IL-6 family cytokines and RANKL *in vitro*. STAT3 inhibition was also effective in treating an RA model, collagen-induced arthritis, *in vivo* through significant reduction in expression of IL-6 family cytokines and RANKL, inhibiting both inflammation and joint destruction. Leukemia inhibitory factor expression and STAT3 activation by IL-1β were mainly promoted by IL-6 but still induced in IL-6-deficient cells. Thus, our data provide new insight into RA pathogenesis and provide evidence that inflammatory cytokines trigger a cytokine amplification loop via IL-6–STAT3 that promotes sustained inflammation and joint destruction.

Keywords: chronic inflammation, collagen-induced arthritis, IL-6, joint destruction, rheumatoid arthritis

Introduction

Rheumatoid arthritis (RA) is a disease characterized by chronic inflammation and joint damage causing joint destruction, which limits patients' daily living activities due to impaired physical function and joint pain. RA is a complex disease resulting from known and unknown factors; however, it is primarily characterized by the presence of major pro-inflammatory cytokines, such as IL-1β, tumor necrosis factor alpha (TNFα) and IL-6. Indeed, the therapeutic antibodies or inhibitors of these inflammatory cytokines provide dramatic therapeutic effects in inhibiting disease activity. Nonetheless, some patients remain resistant to therapy, suggesting that targeting these cytokines individually is not sufficient to treat the pathogenesis of RA.

To date, various RA animal models such as transgenic mice over-expressing IL-1α (IL-1α Tg) or TNFα Tg, mice homozygous for a gp130 F759 mutation, collagen-induced arthritis (CIA) model and antibody against type2 collagen injection model reportedly exhibit RA-like phenotypes, including swelling and destruction in multiple joints (1–5). Analysis of these models indicates that increased serum pro-inflammatory cytokines, activation of inflammatory cells such as macrophages, neutrophils or $CD4^+$ T cells or elevated levels of auto-antibodies underlie RA pathogenesis. Hirano's group reported that an IL-17A-triggered positive feedback loop of IL-6 signaling, which activates both the nuclear factor kappa B (NFκB) and the signal transducer and activator of transcription 3 (STAT3),

promotes autoimmune disease such as encephalomyelitis (6). Recently, they reported that local microbleeding induces an IL-17A-dependent IL-6 amplification loop by inducing local T_h17 accumulation followed by T_h17-mediated IL-6 expression and STAT3 activation in type I collagen-expressing cells (7). However, how inflammation and joint damage are sustained in a chronic manner or why a biological agent inhibiting a single pro-inflammatory cytokine occasionally fails to antagonize disease activity remains unknown.

STAT proteins are a family of transcriptional factors consisting of six members, STATs 1–6, all of which are activated by cytokine stimulation via Janus kinase (Jak) family proteins (8). In mice, STAT3 is implicated in development of visceral endoderm, and STAT3-null mice exhibit early embryonic lethality due to impaired mesoderm formation (9). Jak family proteins are non-receptor type tyrosine kinases consisting of Jak1, Jak2 and Jak3, which transduce various cytokine signals, including IL-6 family cytokines. Phenotypes seen in null mutants of each Jak gene differ, suggesting that each Jak has a unique function. CP690,550 is a small molecule, which was originally developed as a specific inhibitor of Jak3 (10). CP690,550 was utilized as an immunosuppressive agent for organ transplantation (10) and is now in clinical trials as treatment for RA patients (11). CP690,550 has also been utilized in an animal RA model and shown to reduce disease activity *in vivo* (12, 13).

RA causes induction of osteoclast formation, and osteoclasts are implicated in joint destruction due to their bone resorption activity at sub-chondral bone sites (14). Osteoclastogenesis is induced by the cytokine receptor activator of nuclear factor kappa B ligand (RANKL) (15), while osteoclast differentiation is driven by pro-inflammatory cytokines TNFα or IL-1β. Given their unique role in bone resorption, controlling osteoclast activity is considered crucial to prevent joint destruction in RA.

In the current study, we demonstrate that the major inflammatory cytokines elevated in RA, IL-1β, TNFα and IL-6, all function in an amplification circuit for IL-6 family cytokines and RANKL via direct or indirect activation of STAT3. STAT3 activation further induced IL-6 family cytokines as well as RANKL, and lack of STAT3 abrogated both IL-6 family cytokine and RANKL expression. Pharmacological inhibition of STAT3 also inhibited expression of IL-6 family cytokines and RANKL in osteoblastic cells induced by IL-1β, TNFα and IL-6 *in vitro* as well as in the joints of a CIA model *in vivo*. Furthermore, CIA-induced joint swelling and osteoclastogenesis were significantly inhibited by STAT3 abrogation, promoting significant improvements in arthritis scores in the CIA model. These findings indicate that STAT3 is a potential therapeutic target to prevent chronic inflammation and joint destruction in RA.

Methods

Mice

C57B6 mice and DBA/1J mice were purchased from Nihon Jikken Doubutsu (Tokyo, Japan). Animals were maintained under specific pathogen-free conditions in animal facilities certified by the Keio University School of Medicine animal care committee. Animal protocols were approved by the Keio University School of Medicine animal care committee.

CIA model

The experimental CIA model was generated in 6-week-old male mice by injecting 100 μl of emulsion containing 100 μg of type II collagen (CII) (Collagen Research Center, Tokyo, Japan) intradermally at the base of the tail. The basic emulsion was composed of 1 mg ml^{-1} bovine CII dissolved in PBS and an equal volume of complete Freund's adjuvant (Difco, Detroit, MI, USA). Three weeks later, a second immunization containing CII and Incomplete Freund's adjuvant (Difco) was administered. Then, clinical symptoms of arthritis were evaluated visually in each limb and graded on a scale of 0–4; 0, no erythema or swelling; 0.5, swelling of one or more digits; 1, erythema and mild swelling of the ankle joint; 2, mild erythema and mild swelling involving the entire paw; 3, erythema and moderate swelling involving the entire paw and 4, erythema and severe swelling involving the entire paw. The clinical score for each mouse was the sum of the scores for all four limbs (maximum score 16).

Chemicals and reagents

CP-690550 was purchased from Selleck Chemicals (Houston, TX, USA). Cycloheximide was purchased from Sigma–Aldrich (St Louis, MO, USA); mouse IL-1β, mouse TNFα and mouse IL-6 were purchased from PeproTech Ltd (London, UK). Mouse oncostatin M (OSM) and sIL-6Rα were purchased from R&D systems (Minneapolis, MN, USA).

Cell culture

Primary osteoblasts (POBs) derived from calvaria of newborn mice were prepared as described (16, 17). POBs and MC3T3-E1 cells were maintained in αMEM (Sigma–Aldrich) containing 10% fetal bovine serum (FBS) (JRH Biosciences, KS, USA) with penicillin G and streptomycin. Splenocytes and lymphocytes were cultured in RPMI 1640 (Wako Pure Chemicals Industries, Osaka, Japan) supplemented with 10% FBS, 2-mercaptoethanol (Nacalai Tesque, Kyoto, Japan), penicillin G and streptomycin.

In vitro osteoclast formation

BM cells isolated from long bones (femurs and tibias) were cultured for 72 h in αMEM containing 10% heat-inactivated FBS and GlutaMax supplemented with macrophage colony stimulating factor (M-CSF) (50 ng ml^{-1}; Kyowa Hakko Kirin Co.). Adherent cells were then collected for analysis. Cells (10^5) were cultured in 96-well plates with M-CSF and recombinant soluble RANKL (25 ng ml^{-1}; PeproTech Inc.) for 6 days. Osteoclastogenesis was evaluated by tartrate resistance acid phosphatase (TRAP) and May-Grünwald Giemsa staining (18, 19). For co-cultivation, M-CSF-dependent osteoclast progenitor cells and POBs were seeded at a density of 5×10^5 cells and 2×10^4 cells per 48-well plate, respectively, and co-cultured for 7 days in the presence of 50 ng ml^{-1} OSM (R&D) or 10^{-8} M $1,25(OH)_2D_3$ (Wako) plus 1 μM prostaglandin E2 (PGE2) (Wako).

Enzyme-linked immunosorbent assay

ELISA assays for IL-6, IL-17 and IFNγ were undertaken following the manufacturer's instructions (eBioscience, San Diego,

CA, USA). A pSTAT3 ELISA kit (R&D) was utilized to measure pSTAT3 levels according to manufacturer's instructions. The optical density at 450 nm was read on a Labsystems Multiscan MS (Analytical Instruments, LLC, MN, USA).

Real-time PCR analysis

Total RNAs were isolated from cultures or tissues using TRIzol reagent (Invitrogen, Tokyo, Japan). After denaturation of total RNAs at 70°C for 5 min, cDNAs were synthesized by reverse transcription from total RNA using oligo (dT) primer (Wako). Real-time PCR was performed using SYBR Premix ExTaq II (Takara Bio Inc., Shiga, Japan) with the DICE Thermal cycler (Takara Bio Inc.), according to the manufacturer's instructions. Samples were matched to a standard curve generated by amplifying serially diluted products using the same PCR reactions. *β-actin* expression served as an internal control. Primer sequences were as follows:

β-actin forward: 5′-TGAGAGGGAAATCGTGCGTGAC-3′; *β-actin* reverse: 5′-AAGAAGGAAGGCTGGAAAAGAG-3′; *IL-6* forward: 5′-CAAAGCCAGAGTCCTTCAGAG-3′; *IL-6* reverse: 5′-GTCCTTAGCCACTCCTTCTG-3′; *OSM* forward: 5′-AACTCTTCCTCTCAGCTCCT-3′; *OSM* reverse: 5′-TGTGTTCAGGTTTTGGAGGC-3′; *IL-11* forward: 5′-TGGGACATTGGGATCTTTGC-3′; *IL-11* reverse: 5′-CATTGTACATGCCGGA-GGTAG-3′; *Leukemia inhibitory factor (LIF)* forward: 5′-TTCCCATCACCCCTGTAAATG-3′; *LIF* reverse: 5′-GAAACGGCTCCCCTTGAG-3′; *RANKL* forward: 5′-CAATGGCTGGCTTGGTTTCATAG-3′; *RANKL* reverse: 5′-CTGAACCAGACATGACAGCTGGA-3′; *Ctsk* forward: 5′-ACGGAGGCATTGACTCTGAAGATG-3′; *Ctsk* rev-erse: 5′-GGAAGCACCAACGAGAGGAGAAAT-3′; *c-Fos* forward: 5′-ATCGGCAGAAGGGGCAAAGTAG-3′; *c-Fos* reverse: 5′-GCAACGCAGACTTCTCATCTTCAAG-3′; *NFATc1* forward: 5′-CAAGTCTCACCACAGGGCTCACTA-3′; *NFATc1* reverse: 5′-GCGTGAGAGGTTCATTCTCCAAGT-3′

Immunoblotting analysis

Whole-cell lysates were prepared from cultures using radioimmunoprecipitation assay buffer (1% Triton X-100, 1% sodium deoxycholate, 0.1% SDS, 150 mM NaCl, 10 mM Tris–HCl, pH 7.5, 5 mM EDTA and a protease inhibitor cocktail; Sigma–Aldrich). Equivalent amounts of protein were separated by SDS–PAGE and transferred to a PVDF membrane (Millipore, Billerica, MA, USA). Proteins were detected using the following antibodies: anti-pSTAT3 (#9131; Cell signaling technology, Inc., Beverly, MA, USA), anti-STAT3 (sc483; Santa Cruz Biotechnology, Inc., California, USA) and anti-actin (A2066; Sigma–Aldrich).

Histopathology and fluorescent immunohistochemistry

The lower ankle of CIA mice was fixed in 10% neutral-buffered formalin, decalcified in 10% EDTA, pH7.4, embedded in paraffin and then cut into 4-μm sections. Hematoxylin and eosin (H&E) and safranin-O stain were performed according to standard procedures. For each fluorescent immunohistochemistry assay, 4-μm sections were cut and subjected to microwave treatment for 5 min in 1 mM EDTA (pH 8.0) for antigen retrieval. After blocking with 0.1% BSA in 100 mM Tris–HCl (pH 7.6), 150 mM NaCl, 0.01% Tween-20 (TBST) for20 min, sections were stained for 1 h with mouse anti-rabbit pSTAT3 (1:100 dilution; Cell Signaling Techniques, Inc.), goat anti-mouse RANKL (1:150 dilution; R&D Systems, Inc.) or rabbit anti-mouse cathepsin K (1:100 dilution) at room temperature. After washing in TBST, sections were stained with Alexa Fluor 488-conjugated goat anti-mouse IgG (1:200 dilution; Invitrogen), Alexa Fluor 488-conjugated donkey anti-goat IgG (1:200 dilution; Invitrogen) or Alexa Fluor 546-conjugated rabbit anti-mouse IgG (1:200 dilution; Invitrogen) for 1 h at room temperature. Then, sections were mounted using Dako fluorescence mounting medium (Dako, Glostrup, Denmark). TOTO3 (1:750; Invitrogen) was used for a nuclear stain. Images were acquired with a laser confocal microscope (FV1000-D; Olympus, Tokyo, Japan).

Surface and intracellular cytokine staining

For intracellular cytokine staining, cultured cells were restimulated for 8 h with 50 nM phorbol myristate acetate (Sigma–Aldrich), 1 μg ml^{-1} ionomycin (Sigma–Aldrich) and 1 μM brefeldin A (eBioscience). Surface staining was performed for 15 min with the corresponding mixture of fluorescently labeled antibodies as previously described (20). After surface staining, cells were suspended in fixation buffer (eBioscience), and intracellular cytokine staining was performed using the manufacturer's protocol using anti-IL-17-PE (BD Pharmingen). Stained cells were analyzed with BD FACSAria2 (BD Biosciences).

Naive T-cell preparation and differentiation

For naive T-cell preparation and differentiation, $CD4^+CD25^-$ T cells were isolated from wild-type mouse spleens and lymph nodes by negative selection using biotinylated anti-CD25 (clone, BC96; eBioscience), CD8 (clone, 53–6.7; eBioscience), CD11b (clone, M1/70; eBioscience), B220 (clone, RA3-6B2; eBioscience), anti-NK1 1 (PK136; eBioscience), CD11c (N418; eBioscience) followed by streptoavidin-conjugated magnetic beads (Miltenyi Biotech, Bergisch Gladbach, Germany). For T_h17 differentiation, 1×10^6 $CD4^+CD25^-$ T cells were cultured with 1 μg ml^{-1} plate-bound anti-CD3 antibody (clone, 145-2C11; eBioscience), 0.5 μg ml^{-1} soluble anti-CD28 antibody (clone, 37.51; eBioscience), 10 μg ml^{-1} anti-IFN-γ antibody (clone, R4-6A2; PeproTech Inc.), 10 μg ml^{-1} anti-IL-4 antibody (clone, 11B11; PeproTech Inc.), 0.2 ng ml^{-1} recombinant murine IL-2 (PeproTech Inc.), 2 ng ml^{-1} recombinant human transforming growth factor (TGF)-β1 (R&D Systems, Inc.) and 20 ng ml^{-1} recombinant human IL-6 (R&D Systems, Inc.) for 3 days.

Results

IL-1β and TNFα activate STAT3 indirectly

In RA, high levels of inflammatory cytokines such as IL-1β, TNFα and IL-6 are detected and have been targeted by therapeutic antibodies or receptor antagonists (21–23). We found that treatment of osteoblastic cells with IL-1β further stimulated expression of various cytokines, particularly IL-6 family members such as IL-6, OSM, IL-11 and LIF, as well as RANKL, an essential cytokine for differentiation of osteoclasts (Fig. 1A and data not shown). IL-6 family cytokines

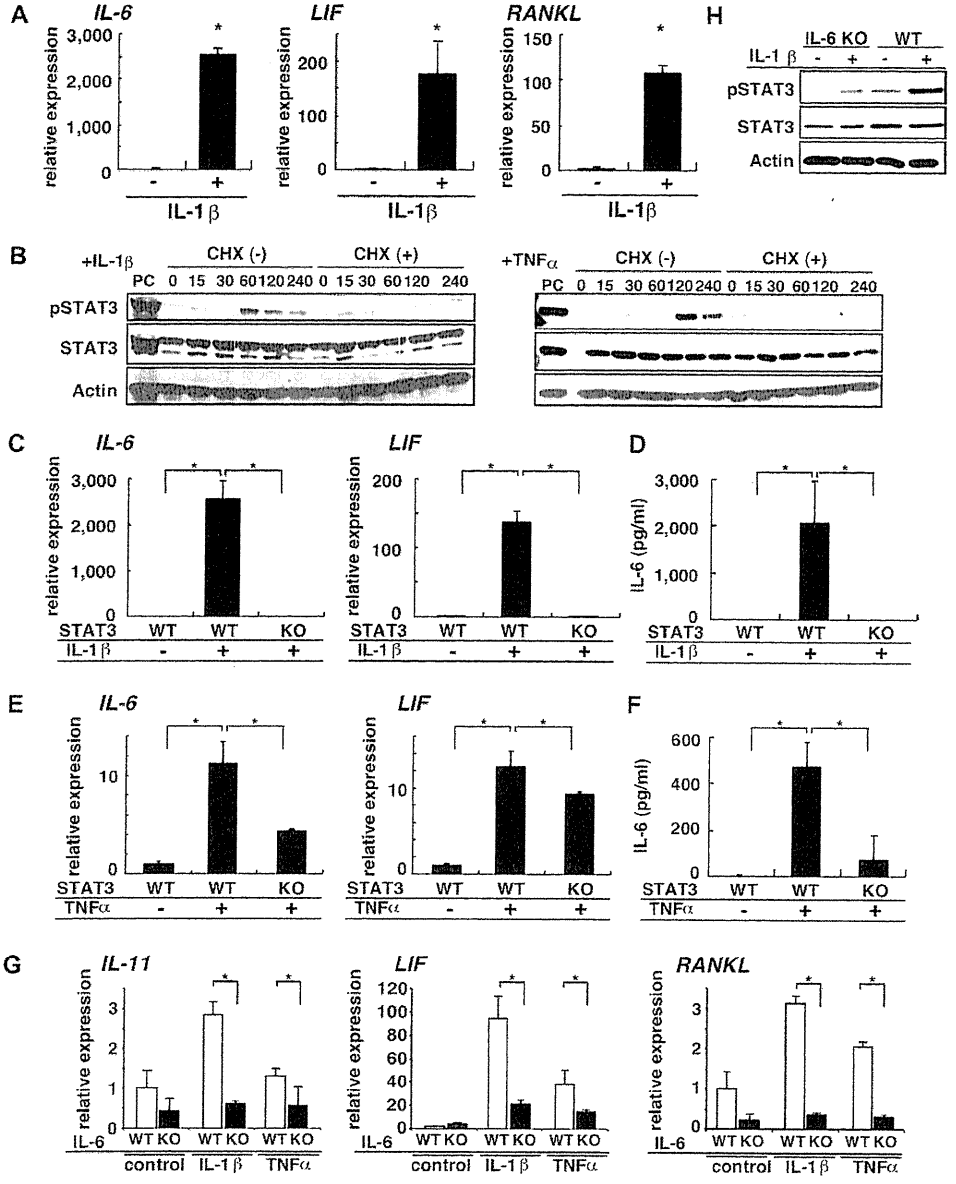

Fig. 1. IL-1β and TNFα stimulation induces IL-6 cytokine family and RANKL expression via STAT3 phosphorylation. (A) Total RNA was prepared from primary mouse osteoblasts treated with (+) or without (−) IL-1β (10 ng ml^{-1}), and expression of the IL-6 cytokine family genes IL-6, LIF, and RANKL relative to β-actin was analyzed by a quantitative real-time PCR. Data are means ± SD of the indicated genes/β-actin (*$P < 0.001$; $n = 3$). (B) Whole-cell lysates from MC3T3-E1 cells stimulated for the indicated times (minute) with IL-1β (10 ng ml^{-1}) or TNFα (10 ng ml^{-1}) in the presence or absence of cycloheximide (CHX, 20 μg ml^{-1}) were analyzed by immunoblotting to detect pSTAT3 and STAT3. Actin served as internal control. (C, E and G) Total RNA was prepared from wild-type (WT), STAT3 KO (KO) or IL-6 KO (KO) MEFs treated with (+) or without (−) IL-1β (10 ng ml^{-1}) or TNFα (10 ng ml^{-1}) for 24 h, and *IL-6*, *LIF*, *IL-11* or *RANKL* expression relative to *β-actin* was analyzed by a quantitative real-time PCR. Data are means ± SD of the indicated genes/*β-actin* (*$P < 0.001$; $n = 3$). (D and F) IL-6 levels in supernatants of WT and STAT3 KO MEFs treated with (+) or without (−) IL-1β (10 ng ml^{-1}) or TNFα (10 ng ml^{-1}) for 24 h were assessed by ELISA. (H) Whole-cell lysates from WT or KO MEFs stimulated for 60 min with IL-1β (10 ng ml^{-1}) were analyzed by immunoblotting to detect pSTAT3 and STAT3. Actin served as internal control.

and RANKL play a crucial role in inflammation and joint destruction, respectively. TNFα and IL-6 treatment also induced expression of these cytokines in osteoblastic cells (Supplementary Figure 1A and B is available at *International Immunology* Online), suggesting that inflammatory cytokines detected in RA trigger further expression of IL-6 family cytokines and RANKL in an autocrine/paracrine amplification manner. Interestingly, although STAT3 is not known to be a direct target of IL-1β and TNFα, STAT3 phosphorylation was induced in osteoblastic cells by IL-1β or TNFα treatment (Fig. 1B). However, STAT3 phosphorylation was strongly inhibited by pre-treatment of cells with cycloheximide, a protein synthesis inhibitor, suggesting that IL-1β and TNFα induce STAT3 indirectly (Fig. 1B). Indeed, we observed direct

activation of IL-1β targets, such as JNK and NF-κB, prior to activation of STAT3 (data not shown), while IL-6 induced STAT3 phosphorylation at an early period (data not shown). These data suggest that major inflammatory cytokines up-regulated in RA, namely IL-1β, TNFα and IL-6, induce STAT3 phosphorylation but that IL-1β and TNFα likely induce STAT3 phosphorylation via IL-6.

We then asked whether STAT3 is required for IL-6-related cytokine induction by IL-1β or TNFα. Expression of IL-6 family cytokines following IL-1β, TNFα or IL-6 stimulation was dramatically inhibited in STAT3-deficient cells (Fig. 1C and E and data not shown). IL-6 protein expression induced by IL-1β and TNFα was also significantly inhibited in STAT3-deficient cells (Fig. 1D and F). IL-6 was implicated in the pathogenesis of RA as an amplifier of cytokines (6), and indeed, the expression of IL-6 family cytokines such as *IL-11* and *LIF* as well as *RANKL* by IL-1β or TNFα was significantly inhibited in IL-6 KO MEFs compared with wild-type MEFs (Fig. 1G). However, STAT3 activation by IL-1β was reduced but still detected in IL-6 KO MEFs (Fig. 1H). These results suggest that STAT3 activity stimulates a cytokine amplification loop that promotes sustained inflammation and RANKL expression in RA and that targeting STAT3 could antagonize chronic inflammation and joint destruction.

STAT3 is a therapeutic target in RA

To determine whether inhibition of STAT3 could have a potential benefit in a mouse model of RA, we undertook experiments using the drug CP690,550, a Jak3 inhibitor also known as Tofacitinib. Osteoblastic MC3T3-E1 cells were treated with IL-1β in the presence of indicated concentrations of CP690,550, and STAT3 phosphorylation was analyzed by western blot (Fig. 2A). CP690,550 treatment effectively decreased STAT3 phosphorylation (Fig. 2A). In addition, CP690,550 was further assessed for effects in a CIA model *in vivo* (Fig. 2B) and found effective in treating arthritis based on arthritis score.

CP690,550 treatment of osteoblastic cells significantly inhibited IL-1β-induced IL-6 family cytokine expression dose-dependently manner *in vitro* (Supplementary Figure 2A is available at *International Immunology* Online). *IL-6* mRNA expression in osteoblastic cells induced by TNFα, IL-6 or OSM was also significantly inhibited by CP690,550 dose dependently (Fig. 2D and Supplementary Figure 2B is available at *International Immunology* Online). Furthermore, IL-6 protein expression induced by IL-1β or TNFα was significantly inhibited by CP690,550 dose dependently (Fig. 2E). These results suggest that STAT3 is the therapeutic target of CP690,550 in blocking a cytokine amplification loop and thereby inhibits sustained inflammation.

Inhibiting STAT3 reduces inflammation seen in a mouse model of RA

To determine whether STAT3 inhibition could ameliorate conditions associated with RA, CP690,550 or vehicle was administered to CIA mice by injection after inflammation had occurred. The arthritis score of CIA mice significantly improved following CP690,550 treatment compared with vehicle treatment (Fig. 3A). Treated mice showed serum IL-6 levels that were significantly down-regulated to a basal level (Fig. 3B), and expression of IL-6 family cytokines in joints was also significantly reduced compared with vehicle-treated control mice (Fig. 3C). Immunohistochemical analysis demonstrated improved fibrosis paralleling reduced STAT3 phosphorylation in joints of CP690,550-treated mice (Fig. 3D). Reduced STAT3 phosphorylation in the joints of CP690,550-treated mice compared with that of control mice was confirmed by western blot and ELISA to detect phosphorylated STAT3 (Fig. 3E). In contrast to STAT3, STAT1 and STAT5 activation was not detected in the joints of CIA mice (Supplementary Figure S3A is available at *International Immunology* Online), suggesting that STAT3 is specifically activated under inflammatory conditions in the joints. STAT3 is also reportedly activated by IL-23 in T cells (24), and the IL-23/STAT3 pathway is known to play a role in the pathogenesis of the CIA model (25). STAT3 activation by IL-23 in T cells is also inhibited by CP690,550 (supplementary Figure S3B is available at *International Immunology* Online), further indicating that CP690,550 inhibits STAT3.

Blocking STAT3 inhibits RANKL expression, osteoclastogenesis and joint destruction in RA

Osteoclastogenesis, which is regulated by the cytokine RANKL, is a crucial event in joint destruction in RA. To examine the effect of STAT3 on RANKL expression, we undertook real-time PCR and immunohistochemistry. *RANKL* expression induced by IL-1β and TNFα was significantly inhibited in STAT3-deficient cells than wild-type cells (Fig. 4A and Supplementary Figure 4A is available at *International Immunology* Online). Induction of *RANKL* expression in osteoblastic cells by the inflammatory cytokines IL-1β and TNFα and by IL-6 family cytokines, such as IL-6 and OSM, was also significantly inhibited by CP690,550 dose dependently (Fig. 4B and Supplementary Figure 4B is available at *International Immunology* Online). Osteoclastogenesis induced in co-cultures of bone marrow-derived osteoclast progenitor cells and osteoblastic cells in the presence of OSM, which induces RANKL expression, was significantly inhibited by CP690,550 dose dependently (Fig. 4C). Vitamin D3 (VitD3) plus PGE2 also reportedly induces RANKL expression in osteoblastic cells and can thus induce osteoclastogeneis in a co-culture system of osteoblastic cells with osteoclast progenitors (26, 27). However, unlike OSM-induced osteoclastogenesis, CP690,550 did not inhibit VitD3 + PGE2-induced osteoclastogenesis (Fig. 4C). IL-1β and TNFα are known to activate the NFκB pathway (28, 29), but NFκB activation by IL-1β was not inhibited by CP690,550 (Supplementary Figure 4C is available at *International Immunology* Online). These results suggest that CP690,550 specifically inhibits osteoclastogenesis induced by STAT3-dependent RANKL expression in osteoblastic cells. Indeed, CP690,550 had little ability to inhibit osteoclastogenesis from bone marrow macrophages in the presence of M-CSF plus RANKL without osteoblastic cells and multinuclear TRAP-positive osteoclasts formed even in the presence of CP690,550 (Fig. 4D). *c-Fos* and *NFATc1*, transcription factors essential for osteoclast differentiation, were induced normally even in the presence of CP690,550 (Fig. 4E). These results suggest that the STAT3 plays a limited role in osteoclast differentiation of progenitor cells.

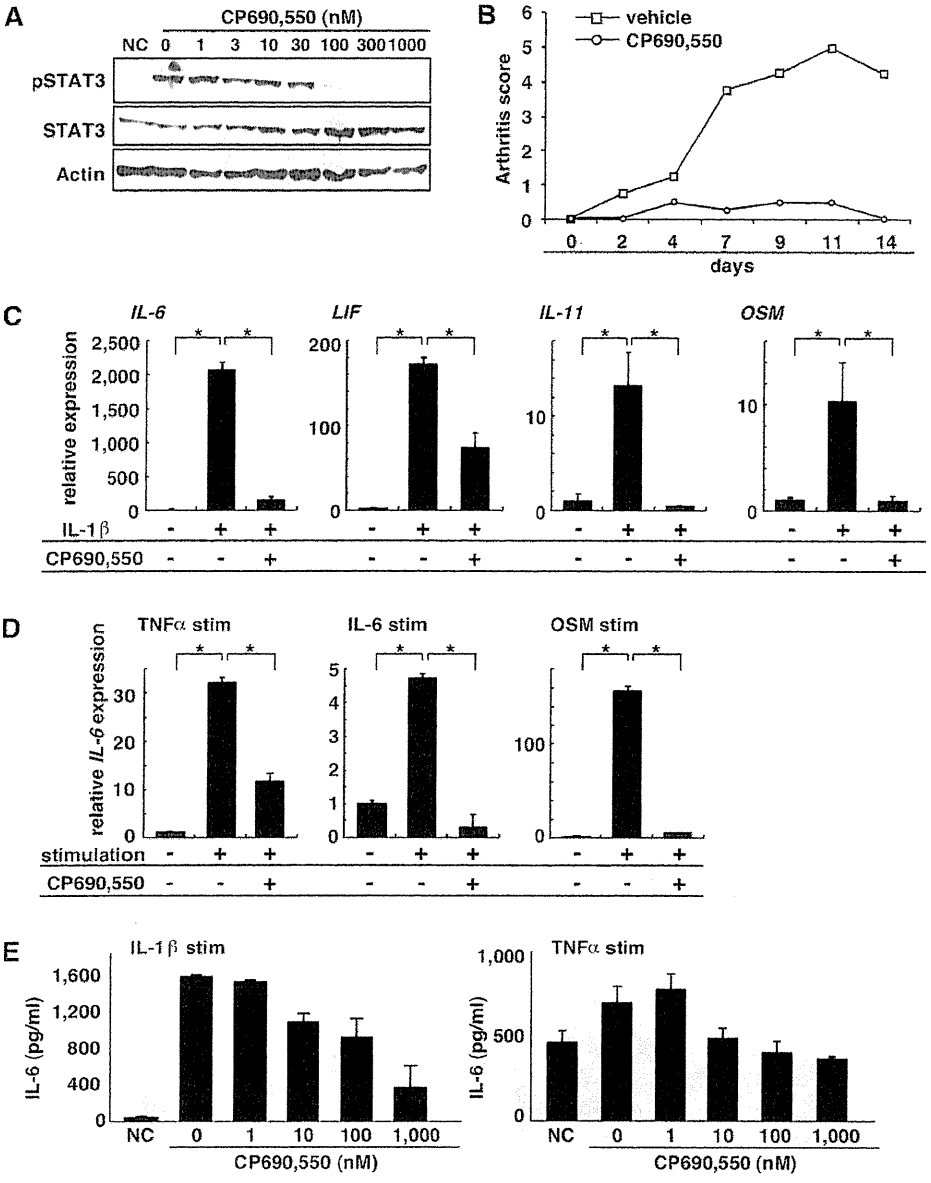

Fig. 2. The STAT3 inhibitor CP690,550 inhibits arthritis in *vivo* and the expression of IL-6 cytokine family *in vitro*. (A) Whole-cell lysates from MC3T3-E1 cells stimulated with IL-1β (10 ng ml^{-1}) plus CP690,550 at the indicated concentrations were analyzed by immunoblotting to detect pSTAT3 and STAT3. Actin served as an internal control. (B) 6-week-old DBA/1 male mice were given an initial injection of type 2 collagen on day −21, and arthritis was induced with a second injection on day 0. Vehicle or CP690,550 (15 mg kg^{-1} day^{-1}) was administered intraperitoneally once daily for 2 weeks from day 0 ($n = 4$ per group). Arthritis scores were measured three times a week. (C and D) Total RNA was prepared from POBs treated with IL-1β (10 ng ml^{-1}), TNFα (10 ng ml^{-1}) or OSM (50 ng ml^{-1}) with (+) or without (−) CP690,550 (100 nM) for 24 h, and *IL-6* expression relative to *β-actin* was analyzed by quantitative real-time PCR. Data are means ± SD of *IL-6/β-actin* (*$P < 0.001$; $n = 3$). (E) IL-6 protein levels in the supernatant of osteoblasts treated with IL-1β (left panel) or TNFα (right panel) plus indicated concentrations of CP690,550 for 24 h were assessed by ELISA. Data are means ± SD of IL-6 (picograms per milliliter).

The mRNA of *RANKL* as well as *Cathepsin K*, an osteoclast differentiation marker, was highly induced in the joints of CIA model but was significantly inhibited by CP690,550 treatment compared with vehicle administration *in vivo* (Fig. 4F). Down-regulated RANKL and cathepsin K expression were also observed in CP690,550-treated CIA mice by immunofluorescence (Fig. 4G). Joint destruction seen in the CIA model was rescued by CP690,550 treatment (Fig. 5). Thus, inhibiting STAT3 in RA can inhibit the inflammatory cytokine loop triggering RANKL expression, thereby inhibiting joint destruction.

Antagonizing STAT3 inhibits differentiation of T_h17 cells

IL-17 producing helper T (T_h17) cells function in the pathogenesis of autoimmune diseases including RA (6, 7). Indeed, T_h17 cells accumulated in regional lymph nodes and

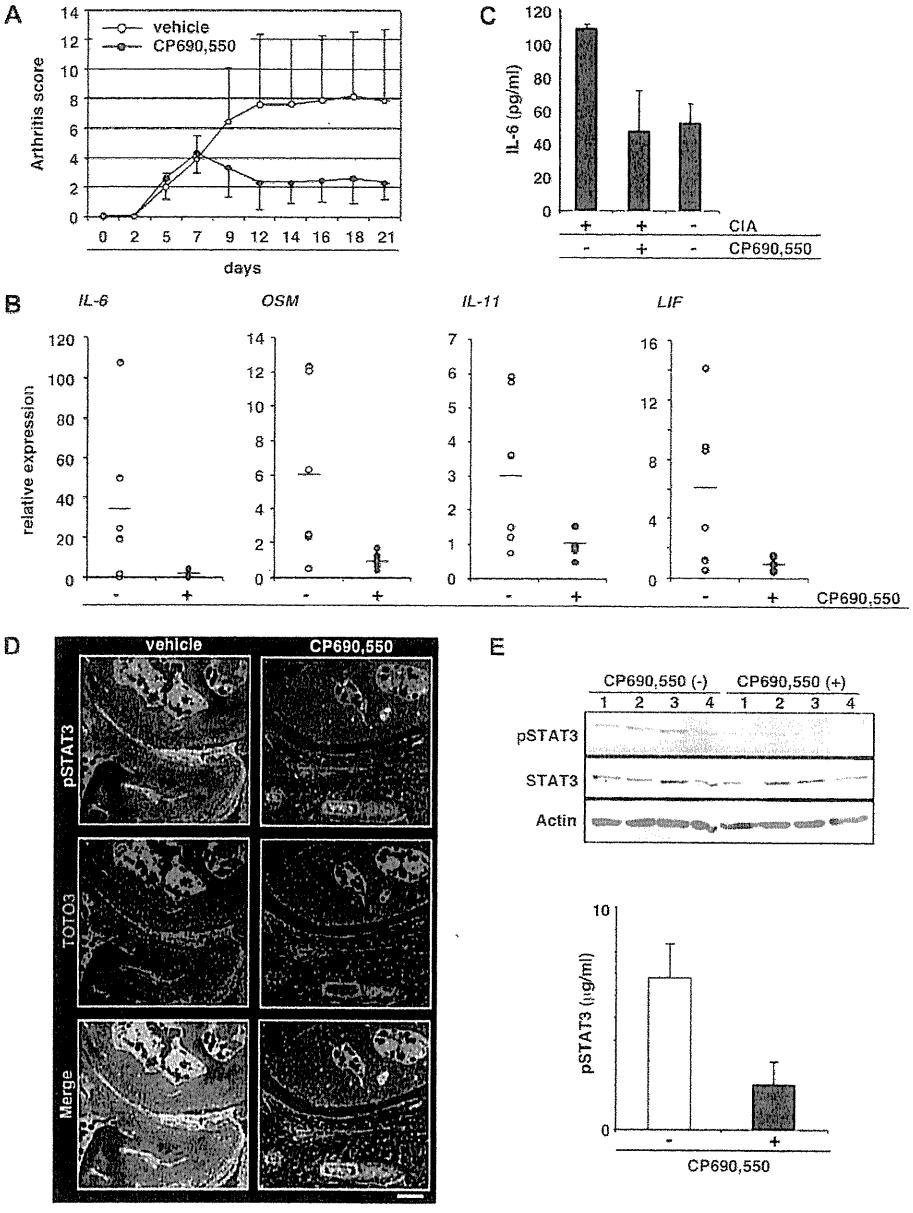

Fig. 3. STAT3 inhibition antagonizes arthritis effects *in vivo*. (A) 6-week-old DBA/J1 male mice were given initial injection of type 2 collagen on day −21, and arthritis was induced with a second injection on day 0. Vehicle or CP690,550 (15 mg kg^{-1} day^{-1}) was administered intraperitoneally once daily for 2 weeks from day 7 (n = 4 per group). Arthritis scores were measured three times a week. (B) Total RNA was prepared from the tissue of hind paws of CIA-induced mice after 2 weeks of treatment by vehicle or CP690,550, and expression of IL-6 cytokine families (*IL-6, OSM, IL-11* and *LIF*) relative to *β-actin* was analyzed by a quantitative real-time PCR. (C) IL-6 serum levels in sera of CIA-induced mice after 2 weeks of treatment by vehicle or CP690,550 were assessed by ELISA. (D) Specimens of ankle joints from CIA mice treated with vehicle or CP690,550 for 2 weeks were subjected to immunofluorescence staining for pSTAT3. Nuclei were visualized by TOTO3. Bar, 100 μm. (E) Whole-cell lysates were made from ankle joint tissues of CIA mice treated with or without CP690,550 for 2 weeks. Phosphorylated STAT3 was then analyzed by western blot (upper panel) and ELISA (lower panel). Results are representative of at least three independent experiments.

spleen of CIA mice, and the appearance of T_h17 cells was slightly but significantly inhibited by CP690,550 treatment *in vivo* (Fig. 6A). In an *ex vivo* assay, IL-17, IL-6 and IFNγ production, which characterizes activation of T cells, induced by T-cell receptor oligomerization by anti-CD3 antibody or type 2 collage treatment was also significantly inhibited in the cells from CP690,550-treated CIA mice (Fig. 6B and data not shown). Interestingly, unlike the *in vivo* and *ex vivo* findings, differentiation of T_h17 cells *in vitro* induced by IL-6 and TGF-β was significantly stimulated by CP690,550 (Fig. 6C). A similar effect was reported by using another JAK inhibitor, pyridone6 (30). This effect was considered due to a more potent effect of the JAK inhibitor on IL-2, IL-4 and IFNγ than on IL-6, resulting in T_h17 differentiation.

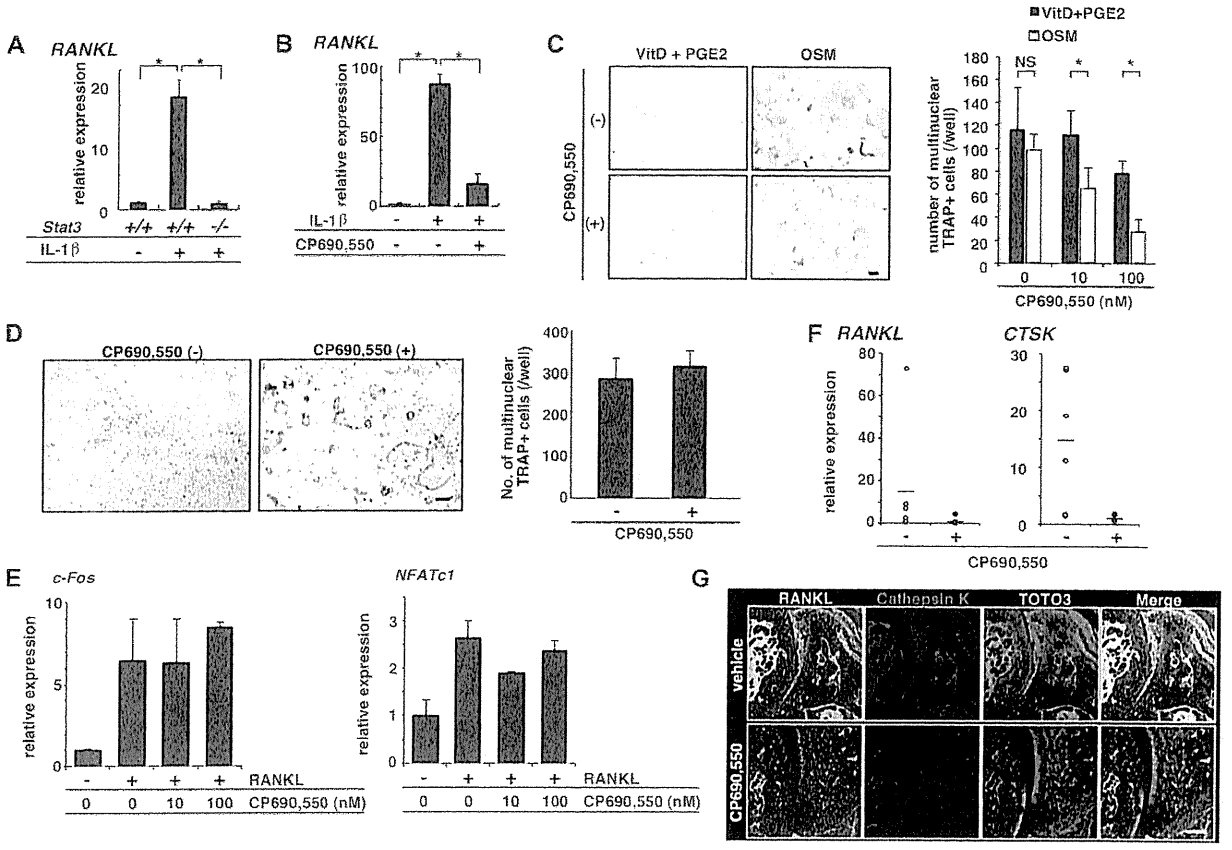

Fig. 4. STAT3 inhibition blocks RANKL expression and osteoclastogenesis *in vivo* and *in vitro*. (A) Total RNA was prepared from wild-type (*+/+*) or STAT3 KO (*–/–*) MEFs treated with (+) or without (–) IL-1β (10 ng ml^{-1}) for 24 h, and expression of *RANKL* relative to *β-actin* was analyzed by quantitative real-time PCR. Data are means ± SD of the *RANKL/β-actin* (*$P < 0.001$; $n = 3$). (B) Total RNA was prepared from wild-type POBs treated with or without IL-1β (10 ng ml^{-1}) in the presence or absence of CP690,550 (100 nM) for 24 h, and expression of *RANKL* relative to *β-actin* was analyzed by quantitative real-time PCR. Data are means ± SD of *RANKL/β-actin* (*$P < 0.001$; $n = 3$). (C) Wild-type POBs and M-CSF-dependent osteoclast progenitor cells were co-cultured in the presence of OSM (50 ng ml^{-1}) or $1,25(OH)_2VitD_3$ (10^{-7} M) + PGE_2 (1 μM) for 7 days, stained with TRAP (left panels) and the number of TRAP-positive cells containing more than three nuclei was scored (right panel) (*$P < 0.001$; $n = 3$). (D and E) M-CSF-dependent osteoclast progenitor cells were cultured in the presence or absence of RANKL (25 ng ml^{-1}) with or without indicated concentrations of CP690,550 for 5 days, stained with TRAP (left) and then the number of multinuclear TRAP-positive cells was scored (right). Data are means ± SD of multinuclear TRAP-positive cells ($n = 6$). Bar, 100 μm. (E) Total RNA was prepared from the above culture, and expression of *c-Fos* and *NFATc1* relative to *β-actin* was analyzed by quantitative real-time PCR. Data are means ± SD of the indicated genes/*β-actin* (*$P < 0.001$; $n = 3$). (F) Total RNA was prepared from hind paw tissues of CIA-induced mice after 2 weeks of treatment by vehicle or CP690,550 (15 mg kg^{-1} day^{-1}), and expression of *RANKL* and *CTSK* relative to β-actin was analyzed by quantitative real-time PCR. (G) Specimens of ankle joints from CIA-induced mice treated with vehicle or CP690,550 for 2 weeks were subjected to immunofluorescence staining for RANKL and CTSK. Nuclei were visualized by TOTO3. Bar, 100 μm. Representatives of at least two independent experiments are shown.

These results suggest that inhibition of T_h17 development by CP690,550 *in vivo* is likely due to IL-6 inhibition. Regulatory T cells (Tregs) are critical to inhibit autoimmune diseases (31), and CP690,550 likely activates Tregs. However, Treg development was inhibited *in vitro* and unchanged *in vivo* following CP690,550 treatment (SupplementaryFigure S5 is available at *International Immunology* Online). Taken together, our data suggests that STAT3 is a critical factor promoting sustained inflammation and osteoclastogenesis leading to chronic inflammation and joint destruction (Fig. 7) and that inhibition of STAT3 activation could constitute a novel anti-RA therapy.

Discussion

RA is a chronic inflammatory disease, which causes continuous joint swelling, pain and damage that limit patients' quality of life (32). To date, various biological agents targeting major pro-inflammatory cytokines up-regulated in RA, such as TNFα, IL-6 and IL-1, have been established, and each of these therapies promotes significant reduction of disease activity (22, 33, 34). However, some populations of RA patients still suffer from continuous inflammation and joint problems (35). Thus, crucial targets to inhibit disease activity in these cases have been sought. Mechanisms underlying sustained inflammation and joint damage in RA remain largely unknown. In this study, we demonstrated that the major pro-inflammatory cytokines in RA, TNFα, IL-6 and IL-1, induced STAT3 activation either directly or indirectly and stimulated expression of IL-6 family cytokines and RANKL in an autocrine/paracrine manner *in vivo* and *in vitro*. Induced IL-6 family cytokines further activated STAT3 and then in turn induced IL-6 family cytokines

and RANKL expression in a cytokine amplification circuit. RANKL induces osteoclastogenesis causing joint destruction by bone resorption. Thus, a loop including inflammatory cytokines, IL-6 family cytokines, RANKL and STAT3 loop likely mediates sustained inflammation and joint destruction in RA. Targeting STAT3 is likely crucial to block that loop.

High expression of inflammatory cytokines or the presence of auto-antibodies and autoreactive lymphocytes is observed and implicated in disease activity in RA and in RA models such as CIA, antigen-induced arthritis. Both were also observed in several reports of spontaneous autoimmune arthritis and in genetically engineered mouse models, including IL-1 Tg, TNF Tg, gp130/F759, ZAP70 SKG and K/BxN (36). In fibroblasts, an IL-17A-triggered positive-feedback loop of IL-6 expression through NFκB and STAT3 activation reportedly promotes arthritis (6), and such IL-17A- and IL-6-dependent arthritis is induced by local events such as microbleeding (7). Indeed, we found that IL-6 expression was significantly down-regulated by STAT3 inhibition caused by gene deletion or CP690,550 treatment in osteoblastic cells, fibroblasts and sera *in vivo*. IL-6 was reported as an amplifier of inflammatory cytokines (6, 7), and we found that STAT3 activation by IL-1 was reduced in IL-6 KO cells, suggesting that STAT3 was mainly activated by IL-6. However, we also found that STAT3 activation was reduced but still induced in IL-6 KO cells, suggesting that STAT3 was also stimulated likely by other IL-6 family cytokines induced by IL-1β, such as LIF, which was up-regulated in IL-6 KO cells by IL-1β or TNFα stimulation (Fig. 1G). In addition, NFκB activation was not inhibited and T_h17 cell development was rather stimulated by CP690,550, suggesting that STAT3 activation described here is, at least in part, IL-17A and IL-6 independent. Thus, we propose that IL-6–STAT3 is a key modulator of RA-related symptoms by inducing cytokine amplification.

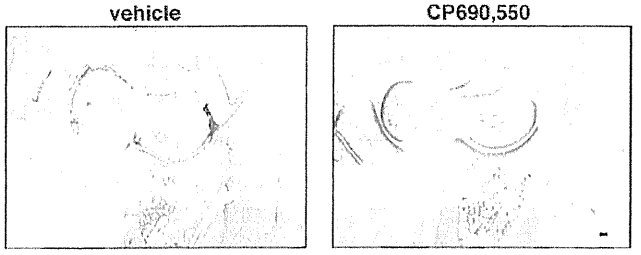

Fig. 5. CP690,550 is effective in treating CIA *in vivo*. 6-week-old DBA/J1 male mice were given an initial injection of type 2 collagen on day −21 and arthritis was induced with a second injection on day 0. Vehicle or CP690,550 (15 mg kg^{-1} day^{-1}) was administered interperitoneally once daily for 2 weeks from day 0 (n = 4 per group). Tissue specimens from the ankle of CIA mice administered vehicle or CP690,550 were stained with safranin O and methyl green. Bar, 100 μm. Representatives of at least two independent experiments are shown.

STAT3 is reportedly a substrate of spleen tyrosine kinase (syk) in B-lineage leukemia/lymphoma cells, and syk is required for oxidative stress-mediated STAT3 activation in tumors (37). A Syk inhibitor was shown to be effective in inhibiting arthritis in the CIA model (38), suggesting that the Syk–STAT3 pathway is likely activated in RA. Inhibitors of Jak1 and Jak2, both upstream of STAT3, effectively improved CIA (39). Furthermore, IL-6 stimulation was shown to induce STAT3 activation as well as complex formation between

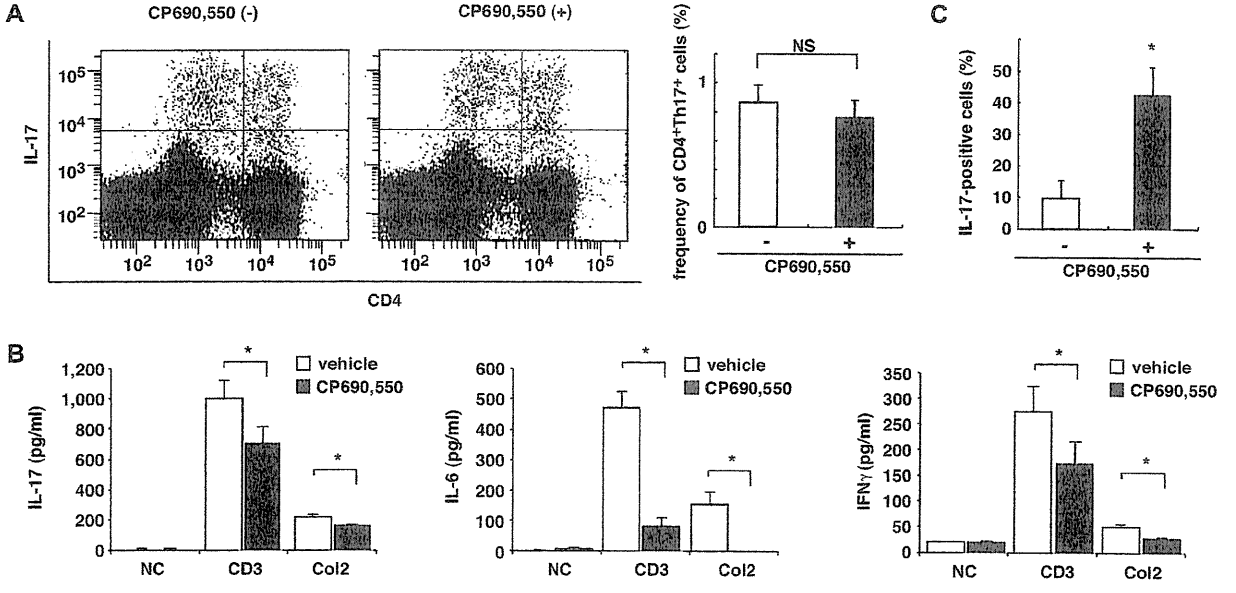

Fig. 6. CP690,550 suppresses T_h17 cells *in vivo* and *ex vivo*. (A) CD4 and intracellular staining of IL-17 in inguinal lymph node cells from CIA-induced mice harvested on day 21 after immunization were examined by flow cytometry (left), and the frequency of CD4+IL-17+ cells (%) was determined (right). (B) Inguinal lymph node cells from CIA-induced mice harvested on day 21 after immunization were cultured with or without anti-CD3 or type 2 collagen (100 μg ml^{-1}) for 5 days, and IL-6, IL-17 and IFNγ levels in the supernatant were assessed by ELISA (*P < 0.001; n = 3). (C) Naive T cells were cultured with 1 μg ml^{-1} plate-bound anti-CD3 antibody (Ab), 0.5 μg ml^{-1} soluble anti-CD28 Ab, 0.2 ng ml^{-1} IL-2, 2 ng ml^{-1} TGF-β1 and IL-6 (20 ng ml^{-1}) in the presence or absence of CP690,550 (50 nM) for 3 days. Foxp3 and IL-17A expression was then analyzed by flow cytometry (*P < 0.001; n = 3). Representatives of at least two independent experiments are shown.

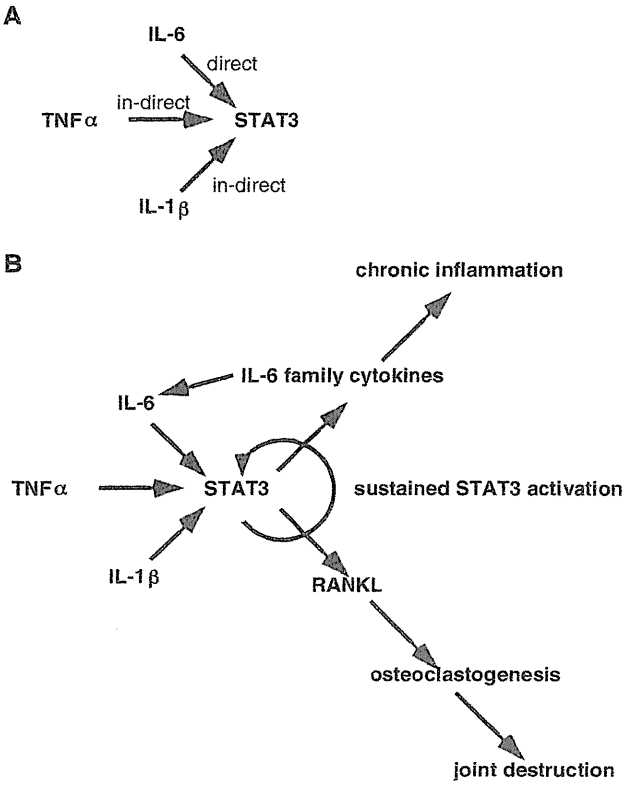

Fig. 7. Scheme of sustained inflammation and joint destruction via STAT3 in RA. (A) Major pro-inflammatory cytokines, namely, IL-6, TNFα and IL-1β, stimulate STAT3 either directly or indirectly. (B) STAT3 activation is followed by expression of IL-6 family cytokines, which in turn induce STAT3 activation in an autocrine/paracrine manner. STAT3 activation further induces RANKL expression, which promotes osteoclastogenesis and joint destruction. Thus, sustained inflammation and joint destruction are developed via STAT3, indicating that STAT3 could be a key target in treating RA.

STAT3 and cyclin-dependent kinase (CDK) 9 (40). Local gene transfer of CDK-inhibitors such as $p16^{INK4a}$ or $p21^{Cip1}$ was also effective in treating CIA (41), suggesting that CDK potentially regulates STAT3 activation.

CP690,550 was originally developed as a Jak3 inhibitor and to a much lesser extent as an inhibitor of Jak1 and Jak2 to mediate immunosuppression (10). The CP690,550 IC50 indicated that it was more effective in inhibiting Jak3 than Jak1 and Jak2 (10, 42). Recently, CP690,550 was also shown to inhibit STAT1 activity (13). In our study, CP690,550 treatment inhibited a cytokine loop via STAT3 inhibition, indicating that STAT3 could be a therapeutic target in chronic inflammatory diseases.

Since IL-6 overproduction has been seen in RA patients and RA models, antagonizing IL-6 activity may be beneficial in treating RA. Indeed, a mAb to IL-6R has proven to be effective against RA. Previously, we reported that over-expression of suppressor of cytokine signaling 3 (SOCS3) or dominant negative STAT3 in joints effectively ameliorated CIA models (43). At that time, we proposed that blocking an intracellular cytokine signaling, particularly JAK1, could be effective against RA treatment. Our study here extends the potential therapeutic effects of JAK–STAT3 inhibitors and shows that they block an inflammatory cytokine-IL-6 circuit that amplifies STAT3 activation.

How does STAT3 contribute to RA? STAT3 has been shown to be necessary for synovial fibroblast proliferation (44), RANKL expression (45), osteoclastegenesis (46) and T_h17 induction (47). We have shown that CP690,550 inhibits many of these effects. Since expression of IL-6, which is required for T_h17 cell development, was significantly inhibited by CP690,550 *in vivo* (Fig. 6A), the reduced frequency of T_h17 cell fraction seen following treatment with CP690,550 *in vivo* is likely due to reduced IL-6 levels caused by the drug. However, the T_h17 cell fraction was enhanced by CP690,550 *in vitro* (Fig. 6C). The precise mechanisms underlying this discrepancy are not clear, but it is likely that CP-690550 inhibits other factors. Indeed, CP690,550 reportedly inhibits other Jaks and STATs (13), and a pan-Jak inhibitor, pyridone6, also stimulates T_h17 development *in vitro* by inhibiting STAT5 (30). Similarly, Treg development *in vitro* was inhibited by CP690,550, and such inhibition is also induced by pyridone6 (30), further suggesting that the *in vitro* effects of CP690,550 on T_h17 and Treg are due, at least in part, to inhibition of Jaks and STATs. Therefore, more specific STAT3 inhibitors are likely required for maximal therapeutic effect.

In RA, osteoclastic bone resorption is frequently elevated and is implicated in joint destruction (14). Some RA patients are treated with steroids, and steroid treatment potently induces osteoporosis, a disease marked by increased osteoclast activity. Thus, control of osteoclastogenesis is crucial for RA patients to avoid joint destruction or drug-induced osteoporosis. RANKL is an essential cytokine for osteoclastogenesis, and RANKL deficiency results in a complete lack of osteoclast formation (48). Thus, RANKL is a target to inhibit osteoclastogenesis in osteoporosis (49) and likely in joint destruction. RANKL expression is reportedly induced by various stimuli such as vitamin D3, parathyroid hormone or IL-6 family cytokines via vitamin D receptor, cyclic adenosine monophosphate or STAT3. In our study, RANKL expression was significantly inhibited in STAT3-deficient cells or in CIA joints of CP690,550-treated mice, suggesting that RANKL expression in RA is regulated by a STAT3-dependent mechanism. Thus, inhibiting STAT3 could benefit to inhibit both inflammation and osteoclastogenesis mediated by an IL-6–STAT3-dependent cytokine loop.

Supplementary data

Supplementary data are available at *International Immunology* Online.

Funding

Special grants-in-aid from the Ministry of Education, Culture, Sports, Science and Technology of Japan, the Japan Society for the Promotion of Science, the Takeda Science Foundation, the Program for the Promotion of Fundamental Studies in Health Science of the National Institute of Biomedical Innovation, the Mochida Memorial Foundation, and the Uehara Memorial Foundation (A.Y.); grant-in-aid for Young Scientists (A) and by Precursory Research for Embryonic Science and Technology, the Takeda Science Foundation and the Keio

Kanrinmaru project, Japan (T.M.); Global Center of Excellence Program at Keio University (T.M.).

Acknowledgements

We thank M. Asakawa, K. Fukuse, N. Shiino, Y. Sato and T. Kobayashi for technical assistance.

References

1 Nixki, Y., Yamada, H., Seki, S. *et al.* 2001. Macrophage- and neutrophil-dominant arthritis in human IL-1 alpha transgenic mice. *J. Clin. Invest.* 107:1127.
2 Keffer, J., Probert, L., Cazlaris, H. *et al.* 1991. Transgenic mice expressing human tumour necrosis factor: a predictive genetic model of arthritis. *EMBO J.* 10:4025.
3 Atsumi, T., Ishihara, K., Kamimura, D. *et al.* 2002. A point mutation of Tyr-759 in interleukin 6 family cytokine receptor subunit gp130 causes autoimmune arthritis. *J. Exp. Med.* 196:979.
4 Trentham, D. E., Townes, A. S. and Kang, A. H. 1977. Autoimmunity to type II collagen an experimental model of arthritis. *J. Exp. Med.* 146:857.
5 Courtenay, J. S., Dallman, M. J., Dayan, A. D., Martin, A. and Mosedale, B. 1980. Immunisation against heterologous type II collagen induces arthritis in mice. *Nature* 283:666.
6 Ogura, H., Murakami, M., Okuyama, Y. *et al.* 2008. Interleukin-17 promotes autoimmunity by triggering a positive-feedback loop via interleukin-6 induction. *Immunity* 29:628.
7 Murakami, M., Okuyama, Y., Ogura, H. *et al.* 2011. Local microbleeding facilitates IL-6- and IL-17-dependent arthritis in the absence of tissue antigen recognition by activated T cells. *J. Exp. Med.* 208:103.
8 Darnell, J. E. Jr. 1997. STATs and gene regulation. *Science* 277:1630.
9 Takeda, K., Noguchi, K., Shi, W. *et al.* 1997. Targeted disruption of the mouse Stat3 gene leads to early embryonic lethality. *Proc. Natl Acad. Sci. USA* 94:3801.
10 Changelian, P. S., Flanagan, M. E., Ball, D. J. *et al.* 2003. Prevention of organ allograft rejection by a specific Janus kinase 3 inhibitor. *Science* 302:875.
11 Coombs, J. H., Bloom, B. J., Breedveld, F. C. *et al.* 2010. Improved pain, physical functioning and health status in patients with rheumatoid arthritis treated with CP-690,550, an orally active Janus kinase (JAK) inhibitor: results from a randomised, double-blind, placebo-controlled trial. *Ann. Rheum. Dis.* 69:413.
12 Milici, A. J., Kudlacz, E. M., Audoly, L., Zwillich, S. and Changelian, P. 2008. Cartilage preservation by inhibition of Janus kinase 3 in two rodent models of rheumatoid arthritis. *Arthritis Res. Ther.* 10:R14.
13 Ghoreschi, K., Jesson, M. I., Li, X. *et al.* 2011. Modulation of innate and adaptive immune responses by tofacitinib (CP-690,550). *J. Immunol.* 186:4234.
14 Bromley, M. and Woolley, D. E. 1984. Chondroclasts and osteoclasts at subchondral sites of erosion in the rheumatoid joint. *Arthritis Rheum.* 27:968.
15 Yasuda, H., Shima, N., Nakagawa, N. *et al.* 1998. Osteoclast differentiation factor is a ligand for osteoprotegerin/osteoclastogenesis-inhibitory factor and is identical to TRANCE/RANKL. *Proc. Natl Acad. Sci. USA* 95:3597.
16 Kosaki, N., Takaishi, H., Kamekura, S. *et al.* 2007. Impaired bone fracture healing in matrix metalloproteinase-13 deficient mice. *Biochem. Biophys. Res. Commun.* 354:846.
17 Matsubara, T., Kida, K., Yamaguchi, A. *et al.* 2008. BMP2 regulates Osterix through Msx2 and Runx2 during osteoblast differentiation. *J. Biol. Chem.* 283:29119.
18 Miyamoto, T., Arai, F., Ohneda, O., Takagi, K., Anderson, D. M. and Suda, T. 2000. An adherent condition is required for formation of multinuclear osteoclasts in the presence of macrophage colony stimulating factor and receptor activator of nuclear factor kappa B ligand. *Blood* 96:4335.
19 Yagi, M., Miyamoto, T., Sawatani, Y. *et al.* 2005. DC STAMP is essential for cell-cell fusion in osteoclasts and foreign body giant cells. *J. Exp. Med.* 202:345.
20 Matsumura, Y., Kobayashi, T., Ichiyama, K. *et al.* 2007. Selective expansion of foxp3-positive regulatory T cells and immunosuppression by suppressors of cytokine signaling 3-deficient dendritic cells. *J. Immunol.* 179:2170.
21 Arend, W. P., Malyak, M., Guthridge, C. J. and Gabay, C. 1998. Interleukin-1 receptor antagonist: role in biology. *Annu. Rev. Immunol.* 16:27.
22 Elliott, M. J., Maini, R. N., Feldmann, M. *et al.* 1994. Randomised double-blind comparison of chimeric monoclonal antibody to tumour necrosis factor alpha (cA2) versus placebo in rheumatoid arthritis. *Lancet* 344:1105.
23 Kishimoto, T. 2005. Interleukin-6: from basic science to medicine—40 years in immunology. *Annu. Rev. Immunol.* 23:1.
24 Mangan, P. R., Harrington, L. E., O'Quinn, D. B. *et al.* 2006. Transforming growth factor-beta induces development of the T(H)17 lineage. *Nature* 441:231.
25 Murphy, C. A., Langrish, C. L., Chen, Y. *et al.* 2003. Divergent pro- and antiinflammatory roles for IL-23 and IL-12 in joint autoimmune inflammation. *J. Exp. Med.* 198:1951.
26 Kitazawa, S., Kajimoto, K., Kondo, T. and Kitazawa, R. 2003. Vitamin D3 supports osteoclastogenesis via functional vitamin D response element of human RANKL gene promoter. *J. Cell. Biochem.* 89:771.
27 Okada, Y., Lorenzo, J. A., Freeman, A. M. *et al.* 2000. Prostaglandin G/H synthase-2 is required for maximal formation of osteoclast-like cells in culture. *J. Clin. Invest.* 105:823.
28 Li, X., Commane, M., Jiang, Z., Stark, G. R. *et al.* 2001. IL-1-induced NFkappa B and c-Jun N-terminal kinase (JNK) activation diverge at IL-1 receptor-associated kinase (IRAK). *Proc. Natl Acad. Sci. USA* 98:4461.
29 Seitz, C., Muller, P., Krieg, R. C. *et al.* 2001. A novel p75TNF receptor isoform mediating NFkappa B activation. *J. Biol. Chem.* 276:19390.
30 Matsunaga, Y., Inoue, H., Fukuyama, S. *et al.* 2011. Effects of a Janus kinase inhibitor, pyridone 6, on airway responses in a murine model of asthma. *Biochem. Biophys. Res. Commun.* 404:261.
31 Kumar, V., Stellrecht, K., Sercarz, E. *et al.* 1996. Inactivation of T cell receptor peptide-specific CD4 regulatory T cells induces chronic experimental autoimmune encephalomyelitis (EAE). *J. Exp. Med.* 184:1609.
32 Scott, D. L., Wolfe, F. and Huizinga, T. W. 2010. Rheumatoid arthritis. *Lancet* 376:1094.
33 Choy, E. H., Isenberg, D. A., Garrood, T. *et al.* 2002. Therapeutic benefit of blocking interleukin-6 activity with an anti-interleukin-6 receptor monoclonal antibody in rheumatoid arthritis: a randomized, double-blind, placebo-controlled, dose-escalation trial. *Arthritis Rheum.* 46:3143.
34 Jiang, Y., Genant, H. K., Watt, I. *et al.* 2000. A multicenter, double-blind, dose-ranging, randomized, placebo-controlled study of recombinant human interleukin-1 receptor antagonist in patients with rheumatoid arthritis: radiologic progression and correlation of Genant and Larsen scores. *Arthritis Rheum.* 43:1001.
35 Buch, M. H., Bingham, S. J., Bryer, D. and Emery, P. 2007. Long-term infliximab treatment in rheumatoid arthritis: subsequent outcome of initial responders. *Rheumatology (Oxford)* 46:1153.
36 Asquith, D. L., Miller, A. M., McInnes, I. B. and Liew, F. Y. 2009. Animal models of rheumatoid arthritis. *Eur. J. Immunol.* 39:2040.
37 Uckun, F. M., Qazi, S., Ma, H., Tuel-Ahlgren, L. and Ozer, Z. 2010. STAT3 is a substrate of SYK tyrosine kinase in B-lineage leukemia/lymphoma cells exposed to oxidative stress. *Proc. Natl Acad. Sci. USA* 107:2902.
38 Konda, V. R., Desai, A., Darland, G., Bland, J. S. and Tripp, M. L. 2010. META060 inhibits osteoclastogenesis and matrix metalloproteinases *in vitro* and reduces bone and cartilage degradation in a mouse model of rheumatoid arthritis. *Arthritis Rheum.* 62:1683.
39 Fridman, J. S., Scherle, P. A., Collins, R. *et al.* 2010. Selective inhibition of JAK1 and JAK2 is efficacious in rodent models of arthritis: preclinical characterization of INCB028050. *J. Immunol.* 184:5298.
40 Hou, T., Ray, S. and Brasier, A. R. 2007. The functional role of an interleukin 6-inducible CDK9. STAT3 complex in human gamma-fibrinogen gene expression. *J. Biol. Chem.* 282:37091.

41 Nasu, K., Kohsaka, H., Nonomura, Y. *et al.* 2000. Adenoviral transfer of cyclin-dependent kinase inhibitor genes suppresses collagen-induced arthritis in mice. *J. Immunol.* 165:7246.
42 Meyer, D. M., Jesson, M. I., Li, X. *et al.* 2010. Anti-inflammatory activity and neutrophil reductions mediated by the JAK1/JAK3 inhibitor, CP-690,550, in rat adjuvant-induced arthritis. *J. Inflamm. (Lond.)* 7:41.
43 Shouda, T., Yoshida, T., Hanada, T. *et al.* 2001. Induction of the cytokine signal regulator SOCS3/CIS3 as a therapeutic strategy for treating inflammatory arthritis. *J. Clin. Invest.* 108:1781.
44 Krause, A., Scaletta, N., Ji, J. D. and Ivashkiv, L. B. 2002. Rheumatoid arthritis synoviocyte survival is dependent on Stat3. *J. Immunol.* 169:6610.
45 Bishop, K. A., Meyer, M. B. and Pike, J. W. 2009. A novel distal enhancer mediates cytokine induction of mouse RANKl gene expression. *Mol. Endocrinol.* 23:2095.
46 O'Brien, C. A., Gubrij, I., Lin, S. C., Saylors, R. L. and Manolagas, S. C. 1999. STAT3 activation in stromal/osteoblastic cells is required for induction of the receptor activator of NF-kappaB ligand and stimulation of osteoclastogenesis by gp130-utilizing cytokines or interleukin-1 but not 1,25-dihydroxyvitamin D3 or parathyroid hormone. *J. Biol. Chem.* 274:19301.
47 Yang, X. O., Panopoulos, A. D., Nurieva, R. *et al.* 2007. STAT3 regulates cytokine-mediated generation of inflammatory helper T cells. *J. Biol. Chem.* 282:9358.
48 Kong, Y. Y., Yoshida, H., Sarosi, I. *et al.* 1999. OPGL is a key regulator of osteoclastogenesis, lymphocyte development and lymph-node organogenesis. *Nature* 397:315.
49 McClung, M. R., Lewiecki, E. M., Cohen, S. B. *et al.* 2006. Denosumab in postmenopausal women with low bone mineral density. *N. Engl. J. Med.* 354:821.

Published October 17, 2011

Brief Definitive Report

Osteoclasts are dispensable for hematopoietic stem cell maintenance and mobilization

Kana Miyamoto,[1,2] Shigeyuki Yoshida,[3,4] Miyuri Kawasumi,[2] Kazuaki Hashimoto,[1,5] Tokuhiro Kimura,[6] Yuiko Sato,[1,7] Tami Kobayashi,[1,2] Yoshiteru Miyauchi,[1,4] Hiroko Hoshi,[1,4] Ryotaro Iwasaki,[3] Hiroya Miyamoto,[1,4] Wu Hao,[1] Hideo Morioka,[1] Kazuhiro Chiba,[1] Takashi Kobayashi,[2] Hisataka Yasuda,[9] Josef M. Penninger,[10] Yoshiaki Toyama,[1] Toshio Suda,[8] and Takeshi Miyamoto[1,2,4,5,11]

[1]Department of Orthopedic Surgery, [2]Keio Kanrinmaru Project, [3]Department of Dentistry and Oral Surgery, [4]Center for Human Metabolomic Systems Biology, [5]Department of Integrated Bone Metabolism and Immunology, [6]Department of Pathology, [7]Department of Musculoskeletal Reconstruction and Regeneration Surgery, and [8]Department of Cell Differentiation, Keio University School of Medicine, Shinjuku-ku, Tokyo 160-8582, Japan
[9]Bioindustry Division, Oriental Yeast Co., Itabashi-ku, Tokyo 174-8505, Japan
[10]Institute of Molecular Biotechnology of the Austrian Academy of Sciences, 1030 Vienna, Austria
[11]Precursory Research for Embryonic Science and Technology, Japan Science and Technology Agency, Kawaguchi, Saitama 332-0012, Japan

Hematopoietic stem cells (HSCs) are maintained in a specific bone marrow (BM) niche in cavities formed by osteoclasts. Osteoclast-deficient mice are osteopetrotic and exhibit closed BM cavities. Osteoclast activity is inversely correlated with hematopoietic activity; however, how osteoclasts and the BM cavity potentially regulate hematopoiesis is not well understood. To investigate this question, we evaluated hematopoietic activity in three osteopetrotic mouse models: *op/op*, c-Fos-deficient, and RANKL (receptor activator of nuclear factor kappa B ligand)-deficient mice. We show that, although osteoclasts and, by consequence, BM cavities are absent in these animals, hematopoietic stem and progenitor cell (HSPC) mobilization after granulocyte colony-stimulating factor injection was comparable or even higher in all three lines compared with wild-type mice. In contrast, osteoprotegerin-deficient mice, which have increased numbers of osteoclasts, showed reduced HSPC mobilization. BM-deficient patients and mice reportedly maintain hematopoiesis in extramedullary spaces, such as spleen; however, splenectomized *op/op* mice did not show reduced HSPC mobilization. Interestingly, we detected an HSC population in osteopetrotic bone of *op/op* mice, and pharmacological ablation of osteoclasts in wild-type mice did not inhibit, and even increased, HSPC mobilization. These results suggest that osteoclasts are dispensable for HSC mobilization and may function as negative regulators in the hematopoietic system.

CORRESPONDENCE
T. Miyamoto:
miyamoto@z5.keio.jp

Abbreviations used: 5-FU, 5-fluorouracil; BMD, bone mineral density; HSC, hematopoietic stem cell; HSPC, hematopoietic stem and progenitor cell; LSK, lineage negative, c-Kit positive, and Sca1 positive; OPG, osteoprotegerin; RANKL, receptor activator of nuclear factor kappa B ligand.

Hematopoietic stem cells (HSCs) have the ability to self-renew as well as to produce multiple lineages of daughter cells throughout an animal's life (Adams and Scadden, 2006; Kiel and Morrison, 2008). Hematopoietic stem and progenitor cells (HSPCs) are thought to reside in specific niches, which are specialized microenvironments within the BM cavity (Calvi et al., 2003; Zhang et al., 2003; Arai et al., 2004; Kiel et al., 2005; Stier et al., 2005; Adams and Scadden, 2006; Sugiyama et al., 2006; Kiel and Morrison, 2008; Lymperi et al., 2010). Niches consist of various cell types such as osteoblastic cells, vascular endothelial cells or reticular cells, and associated factors such as angiopoietin1, N-cadherin, osteopontin, and Cxcl12 (Calvi et al., 2003; Zhang et al., 2003; Arai et al., 2004; Kiel et al., 2005; Stier et al., 2005; Adams and Scadden, 2006; Sugiyama et al., 2006; Kiel and Morrison, 2008; Lymperi et al., 2010). A functional BM is reportedly required for HSPC mobilization to the periphery from BM cavities (Katayama et al., 2006). Thus, these cavities are considered crucial for HSPC

The Rockefeller University Press $30.00
J. Exp. Med. Vol. 208 No. 11 2175-2181
www.jem.org/cgi/doi/10.1084/jem.20101890

Supplemental Material can be found at:
http://jem.rupress.org/content/suppl/2011/10/13/jem.20101890.DC1.html

Published October 17, 2011

maintenance and mobilization; however, the impact of loss of BM cavities on the hematopoietic system remains unclear.

BM cavities are formed by osteoclasts, which are bone resorbing multinuclear cells, and loss of osteoclasts results in loss of BM cavities (Yoshida et al., 1990; Grigoriadis et al., 1994; Kong et al., 1999). Various factors, such as M-CSF, c-Fos, and receptor activator of nuclear factor kappa B ligand (RANKL), are reportedly essential for osteoclastogenesis; mutational inactivation or genetic ablation of these molecules results in a lack of osteoclast differentiation and consequent defects in BM cavity formation, a condition termed osteopetrosis in which BM cavities are filled with bone (Yoshida et al., 1990; Grigoriadis et al., 1994; Kong et al., 1999). Osteoprotegerin (OPG) is a decoy receptor of RANKL that inhibits osteoclastogenesis (Bucay et al., 1998; Mizuno et al., 1998). Although bone phenotypes of *op/op*, c-Fos–deficient, RANKL-deficient, and OPG-deficient mice have been described, hematopoietic phenotypes in these mice have not yet been fully characterized. Clinically, osteoclastic activity increases after serial G-CSF injection administered before peripheral HSC implantation (Takamatsu et al., 1998; Watanabe et al., 2003), and such activity is reportedly required to drive HSPCs from the marrow to the periphery (Kollet et al., 2006). Therefore osteoclast-deficient mice, which lack a BM niche, are predicted to be defective in hematopoiesis as a result of impaired osteoclast activity required to mobilize HSPCs to the periphery. Indeed, osteopetrotic patients, as well as animal models, reportedly show extramedullary hematopoiesis in the spleen (Freedman and Saunders, 1981; Lowell et al., 1996).

Osteoclastogenesis is accelerated with age, resulting in decreased bone mass (Manolagas and Jilka, 1995; Teitelbaum, 2007). Hematopoietic activity also decreases with age (Geiger and Rudolph, 2009; Waterstrat and Van Zant, 2009), suggesting that osteoclast activity is inversely correlated with hematopoietic activity; however, precise roles of osteoclasts in regulating hematopoiesis are largely unknown.

In this paper, we show that HSPCs are maintained even in osteopetrotic animals and that they are mobilized to the periphery after G-CSF stimulation, indicating that osteoclasts and BM cavities are both dispensable for HSPC maintenance and egress to the periphery. Pharmacological inhibition of osteoclastic activity did not inhibit but rather stimulated HSPC mobilization. Splenectomy of *op/op* mice increased HSPC mobilization, suggesting that spleen is not the primary tissue that maintains HSCs in osteopetrotic animals. HSCs were also detected in the osteopetrotic bone. OPG-deficient mice, which show increased osteoclastic activity, exhibited reduced HSPC mobilization. Thus, accelerated osteoclastic activity decreases both bone mass and hematopoietic activity, and both can be manipulated pharmacologically in vivo.

RESULTS AND DISCUSSION

HSPCs are maintained and mobilized in *op/op* mice

To determine whether loss of the BM niche and osteoclasts influences hematopoiesis, we analyzed osteopetrotic *op/op* mice, which carry a loss-of-function mutation in M-CSF, a cytokine essential for osteoclast differentiation (Yoshida et al., 1990). These mice lack a BM cavity and exhibit impaired osteoclastogenesis (Fig. 1 A). Previously, the cell cycle–specific cytotoxic agent 5-fluorouracil (5-FU), which is used in chemotherapy, has been used to evaluate HSC function because HSCs are resistant to 5-FU–induced cell death as a result of their quiescence (Cheng et al., 2000; Miyamoto et al., 2007). *op/op* and wild-type mice were serially treated with 5-FU, and we found that *op/op* mice were lethally susceptible to 5-FU treatment compared with control *op/+* mice (Fig. 1 B), suggesting that osteoclasts and BM cavities are required to maintain HSCs.

To confirm roles of osteoclasts and BM cavities in the hematopoietic system, *op/op* mice were serially treated with G-CSF and HSPCs mobilization was analyzed (Fig. 1, C–E). Because a functional BM niche or osteoclasts are reportedly required to mobilize HSPCs to the periphery from the BM (Heissig et al., 2002; Katayama et al., 2006; Kollet et al., 2006), we predicted that *op/op* mice would show inhibited HSPC mobilization after G-CSF injection. However, we found that mobilization of the HSC-enriched fraction (lineage negative, c-Kit positive, and Sca1 positive [LSK]) to peripheral blood, as analyzed by flow cytometry, was induced to levels even higher in *op/op* mice than in control littermate mice (*op/+*; Fig. 1, C and D). HSPCs mobilized in *op/op* mice were functional: colony-forming assays showed that greater numbers of colonies formed from the peripheral blood of G-CSF–treated *op/op* mice than from that of wild-type mice (Fig. 1 E). This observation suggests that *op/op* mice accumulate a greater number of HSCs than do wild-type mice, and that neither BM cavities nor osteoclasts are required for HSC maintenance and mobilization and may even be inhibitory to the process.

HSPC mobilization is induced in c-Fos– and RANKL-deficient mice

To confirm these findings, c-Fos–deficient mice, which are also osteoclast deficient and lack BM cavities, were analyzed (Fig. S1 A). We observed that c-Fos–deficient mice were less susceptible to serial 5-FU treatment than were *op/op* mice (Fig. S1 B), suggesting that M-CSF, rather than BM cavities and osteoclasts, is required to resist 5-FU treatment. Indeed, injection of M-CSF into *op/op* mice rescued mice from a lethal response to 5-FU (Fig. S1 C). M-CSF regulates osteoclast formation as well as macrophage differentiation and innate immunity (Miyamoto et al., 2001; Chitu and Stanley, 2006). In wild-type mice, M-CSF concentration in sera was significantly up-regulated after 5-FU treatment, suggesting a protective role for M-CSF against myelosuppression induced by chemotherapy (Fig. S1 D). In fact, both Gram-positive and -negative bacteria were detected in multiple organs of 5-FU–treated *op/op* mice (Fig. S1 E and not depicted). These results indicate that by inducing macrophages, M-CSF likely plays a critical role in resistance to hematopoietic suppression after 5-FU treatment. They also suggest that serum M-CSF concentrations should be carefully monitored during myelosuppressive chemotherapies to prevent opportunistic infections.

Published October 17, 2011

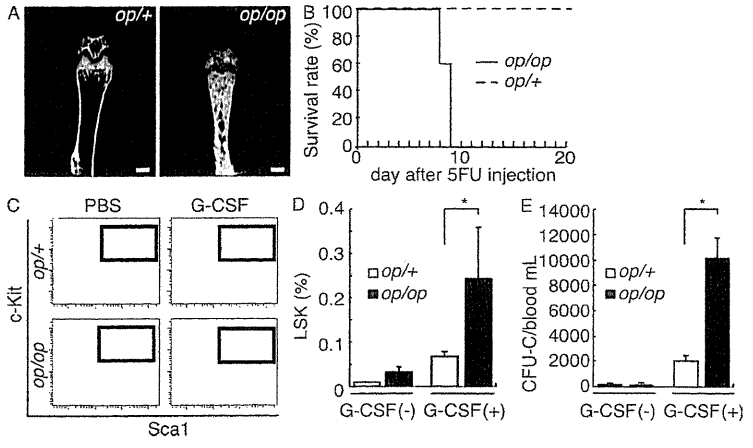

Figure 1. *op/op* mice are osteopetrotic and exhibit increased numbers of HSPCs. (A) Microradiographical analysis of femoral bones of 8-wk-old *op/op* and control (*op/+*) bone. Representative micro-CT data in three independent *op/op* or *op/+* mouse bones are shown. Bars, 1 mm. (B) 150 mg/kg 5-FU was injected into the peritoneal cavity of 8-wk-old *op/op* ($n = 5$) and littermate control (*op/+*; $n = 5$) mice on days 0 and 7, and the survival rate after 5-FU injection was analyzed. (C–E) 250 µg/kg/d G-CSF or PBS was injected subcutaneously into 8–12-wk-old *op/op* and control (*op/+*) mice daily for 5 d ($n = 3$ for each group). Peripheral blood was collected, and the frequency of the HSC fraction (LSK; C and D) and CFU-C (E) were analyzed. (C) Representative flow cytometric pattern of peripheral blood. Cells were gated on lineage (CD3, B220, TER119, Mac1, and Gr1)-negative cells. Data represent the mean LSK frequency (%) ± SD in peripheral blood (*, $P < 0.051$; D) and CFU-C ± SD in 1 ml peripheral blood (*, $P < 0.01$, $n = 9$ for each group; E). Representative data of three independent experiments are shown (B–E).

RANKL-deficient mice are also osteoclast deficient and lack BM cavities (Fig. S1 F). Interestingly, increased HSPC mobilization after serial G-CSF treatment was observed in both c-Fos–deficient and RANKL-deficient mice (Fig. 2), as it was in *op/op* mice, supporting the idea that osteoclasts and BM cavities are not required to maintain HSCs. Young female PTPε-knockout mice reportedly show a mild loss of osteoclast function but exhibit a BM cavity and impaired HSPC mobilization by G-CSF (Kollet et al., 2006). The three osteoclast- and BM cavity–deficient animal models evaluated in this study did not show defective HSPC mobilization after G-CSF treatment, suggesting that the function of osteoclasts in driving HSCs to the periphery is biphasic or BM cavity dependent. In wild-type mice, the number of osteoclasts reportedly does not increase during G-CSF treatment, but only after cessation of treatment (Takamatsu et al., 1998; Christopher and Link, 2008; Winkler et al., 2010), also suggesting that osteoclast loss likely does not affect HSPC mobilization in response to G-CSF treatment. All three osteopetrotic animal models show increased mobilization of HSPCs to the periphery without G-CSF administration (Figs. 1 and 2), suggesting that steady-state levels of circulating HSPCs are increased in these animals.

Impaired HSPC mobilization in OPG-deficient mice

To further explore the role of BM cavities and osteoclasts in HSC maintenance, HSPC mobilization in OPG-deficient mice was analyzed by serial G-CSF injection (Fig. 3). OPG is a decoy receptor for RANKL and therefore acts as a RANKL inhibitor (Bucay et al., 1998; Mizuno et al., 1998). OPG-deficient mice show severe osteoporosis as a result of accelerated osteoclastogenesis (Fig. 3, A and B). As expected, in contrast to osteoclast-deficient osteopetrotic mice, reduced HSPC mobilization was seen in OPG-deficient mice, as indicated by flow cytometry and colony-forming assays, compared with wild-type mice (Fig. 3, C–E). Furthermore, long-term competitive repopulation assays using mobilized cells from CD45.2$^+$ *op/op*, c-Fos–deficient, or RANKL-deficient mice versus CD45.1$^+$ BM competitors showed higher chimerism relative to that induced using mobilized cells from control mice (Fig. 3 F). In contrast, mobilized cells from OPG-deficient mice induced lower chimerism than those from wild-type mice (Fig. 3 F). CD45.2 reconstitution was multilineage; CD45.2 reconstitution from mobilized donor

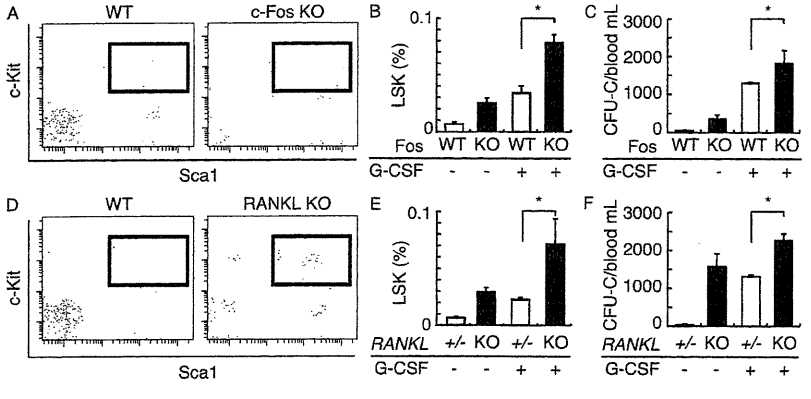

Figure 2. c-Fos–deficient and RANKL-deficient mice show elevated HSPC pools. (A–F) 250 µg/kg/d G-CSF or control PBS was injected subcutaneously into 8–12-wk-old c-Fos–deficient (c-Fos KO; $n = 5$ for each group) or RANKL-deficient (RANKL KO; $n = 5$ for each group) mice or into respective control littermates (wild-type [WT]; $n = 5$ for each group) daily for 5 d. Peripheral blood was collected, and the proportion of HSCs (A, B, D, and E) and CFU-C (C and F) were analyzed. (A and D) Representative flow cytometry pattern of peripheral blood. Cells were gated on lineage-negative cells. Data represent the mean LSK frequency (%) ± SD in peripheral blood (*, $P < 0.01$, $n = 5$ for each group; B and E) and mean CFU-C ± SD in 1 ml peripheral blood (*, $P < 0.01$, $n = 6$ for each group; C and F). Representative data from one of three independent experiments are shown (A–F).